TR-21

DEVELOPMENT OF A VARIABLE PARAMETER SIMPLIFIED HYDRAULIC FLOOD ROUTING MODEL FOR TRAPEZOIDAL CHANNELS

SATISH CHANDRA
DIRECTOR

STUDY GROUP

M PERUMAL

NATIONAL INSTITUTE OF HYDROLOGY
JAL VIGYAN BHAWAN
ROORKEE-247667(UP)
INDIA

1986-87

CONTENTS

		PAGE NO
	LIST OF SYMBOLS	(i)
	LIST OF FIGURES	(iv)
	LIST OF TABLES	(vi)
	ABSTRACT	(vii)
1.0	INTRODUCTION	1
2.0	REVIEW	6
3.0	PROBLEM DEFINITION	15
4.0	METHODOLOGY	16
5.0	APPLICATION	35
6.0	RESULTS AND DISCUSSION	45
7.0	CONCLUSIONS	82
	REFERENCES	85

LIST OF SYMBOLS

A	flow area of the channel at a section
A_m	flow area at mid-section of the routing reach of length Δx
B	channel width
B_m	channelwidth at mid-section of the routing reach of length Δx
C	Chezy's friction coefficient
c	travel speed corresponding to discharge Q at a section
C_1, C_2, C_3	Coefficients of the conventional Muskingum difference equation
EVOL	relative error in flow volume
F	Froude number
F_o	Froude number corresponding to reference discharge Q_o
g	gravity due to acceleration
I_i	the i^{th} inflow discharge
I_p	the inflow hydrograph peak
I_1, I_2	respectively inflow at the beginning and end of the routing time interval
j	notation identifying the location of cross-section in the reach
K	the Muskingum travel time
K_o	the Muskingum travel time corresponding to initial steady flow
ℓ	distance between mid-section and section (3)
n	Manning's coefficient of roughness; also notation identifying the routing time level
Q	discharge at any section of the channel reach during unsteady flow; also discharge at section (2), specifically.

Q_b	base flow
Q_m	discharge at mid-section of the routing reach of length Δx
Q_n	normal discharge
Q_p	peak outflow
Q_o	reference discharge
Q_3	discharge at section (3)
Q_{ci}	the i^{th} computed discharge
Q_{oi}	the i^{th} observed discharge
Q_{PE}	relative error in peak discharge (%)
$\bar{Q}_{oi}$	mean of the observed discharges
S_f	friction slope
S_o	bed slope
t	notation for time
T_{PQE}	error in time of peak discharge
T_{PYE}	error in time of peak stage
$t(y_{pc})$	time corresponding to computed peak stage at the outflow section
$t(y_{po})$	time corresponding to observed peak stage at the outflow section
$t(Q_{pc})$	time corresponding to computed peak discharge
$t(Q_{po})$	time corresponding to observed peak discharge
v	velocity of flow at any section
v_m	velocity of flow at mid-section of the routing reach of length Δx
v_o	velocity corresponding to reference discharge Q_o
v_3	velocity of flow at section (3)
x	notation for distance
y	depth of flow

y_3	depth of flow at section (3)
y_{PE}	error in peak stage
y_m	depth of flow at mid-section of the routing reach of length Δx
y_{pc}	computed peak stage at the outflow section
y_{po}	observed peak stage at the outflow section
Δt	routing time interval
Δx	length of the routing reach
θ	Muskingum weighting parameter
θ_o	θ corresponding to initial steadyflow
τ	dummy time variable
Z	side slope of the trapezoidal cross section of the channel (Z horizontal : 1 vertical)

LIST OF FIGURES

FIGURE	TITLE	PAGE
1.	SPACE TIME DISCRETIZATION OF MUSKINGUM METHOD	10
2.	DEFINITION SKETCH OF THE REACH UNDER CONSIDERATION	19
3.	OBSERVED AND COMPUTED DISCHARGE HYDROGRAPHS FOR CHANNEL TYPE-1	48
4.	OBSERVED AND COMPUTED STAGE HYDROGRAPHS FOR CHANNEL TYPE-1	49
5.	OBSERVED AND COMPUTED DISCHARGE HYDROGRAPHS FOR CHANNEL TYPE-2	50
6.	OBSERVED AND COMPUTED STAGE HYDROGRAPHS FOR CHANNEL TYPE-2	51
7	OBSERVED AND COMPUTED DISCHARGE HYDROGRAPHS FOR CHANNEL TYPE-3	52
8.	OBSERVED AND COMPUTED STAGE HYDROGRAPHS FOR CHANNEL TYPE-3	53
9.	OBSERVED AND COMPUTED DISCHARGE HYDROGRAPHS FOR CHANNEL TYPE-4	54
10.	OBSERVED AND COMPUTED STAGE HYDROGRAPHS FOR CHANNEL TYPE-4	55
11.	VARIATION OF TRAVEL TIME WITH INFLOW FOR CHANNEL TYPE-1	56
12.	VARIATION OF TRAVEL TIME WITH INFLOW FOR CHANNEL TYPE-2	57
13.	VARIATION OF TRAVEL TIME WITH INFLOW FOR CHANNEL TYPE-3	58

14.	VARIATION OF TRAVEL TIME WITH INFLOW FOR CHANNEL TYPE-4	59
15.	VARIATION OF θ WITH INFLOW FOR CHANNEL TYPE-1	60
16.	VARIATION OF θ WITH INFLOW FOR CHANNEL TYPE-2	61
17.	VARIATION OF θ WITH INFLOW FOR CHANNEL TYPE-3	62
18.	VARIATION OF θ WITH INFLOW FOR CHANNEL TYPE-4	63
19.	COMPARISON OF INTERPOLATED HYDROGRAPH AND DIRECTLY ROUTED HYDROGRAPH FOR 5 KM REACH (CHANNEL TYPE-1).	64
20.	COMPARISON OF INTERPOLATED STAGE HYDROGRAPH AND THE STAGE HYDROGRAPH OBTAINED BY DIRECT ROUTING FOR 5 KM REACH (CHANNEL TYPE-1)	65
21.	COMPARISON OF INTERPOLATED HYDROGRAPH AND DIRECTLY ROUTED HYDROGRAPH FOR 5 KM. REACH(CHANNEL TYPE-2).	66
22.	COMPARISON OF INTERPOLATED STAGE HYDROGRAPH AND THE STAGE HYDROGRAPH OBTAINED BY DIRECT ROUTING FOR 5 KM. REACH (CHANNEL TYPE-2)	67
23.	VARIATION OF θ WITH INFLOW FOR THE ROUTING REACH OF 5 KM. (CHANNEL TYPE-1).	68

IST OF TABLES

Table	Title	Page No.
1.	CHANNEL CONFIGURATIONS	37
2.	TEST RUN DETAILS	41
3.	COMPARISON OF RESULTS	46
4.	TYPICAL VALUES OF $\frac{1}{S_o} \cdot \frac{\partial y}{\partial x}$	78

ABSTRACT

A variable parameter simplified hydraulic method based on the approximation of the St.Venant's equations which describe the one dimensional flow in a channel or river has been developed for routing floods in channels having uniform trapezoidal cross section and constant bed slope. The governing equations of this method are same as that of Muskingum flood routing method and it has been demonstrated that these equations can directly account for flood wave attenuation without attributing to it the numerical property of the method as stated by some researchers. The parameters θ and K viz., the weighting parameter and the travel time respectively, have been related to the channel and flow characteristics. Using this method the nonlinear behaviour of flood wave movement may be modelled by varying the parameters θ and K at every routing time level, but still adopting the linear form of solution equation.

The developed method has been applied for routing floods in four different channels having prismatic trapezoidal cross-section with different constant bed slopes and Manning's roughness coefficients, and the results were compared with the corresponding St.Venant's solutions. Three different solution approaches have been used for routing floods in each channel corresponding to a reach length of 40 km. These approaches consists of considering the entire 40 km. length as a single reach and obtaining the solution by varying θ and K; considering

the entire 40 Km. length as a single reach but obtaining the solution by varying K and keeping θ constant; and considering the 40 Km. reach consists of 8 equal sub-reaches and obtaining the solution by successively routing through these reaches by varying both θ and K. It has been found from this study in general, the last solution approach is able to reproduce more closely the St.Venant's solution for both stage and discharge hydrographs, when compared with the other two approaches.

The theoretical reason for the reduced outflow in the beginning of the Muskingum solution has been brought out and the needed remedial measure to avoid it is suggested. Also it has been brought out from theoretical considerations that for Muskingum method, the maximum value of θ is 0.5 and its negative value is admissible.

1.0 INTRODUCTION

Flood routing is the process of tracking a flood wave as it propagates down a channel or a river. A great many different methods and procedures for solving flood routing problems have been described in engineering literature. In general, those methods that attempt a strict mathematical treatment of the many complex factors affecting flood wave movement are not easily adaptable to the practical solution of problems of routing floods as they demand on high computer resources as well as quantity and quality of input data. In order to keep the amount of computation within practical limits and to confirm to limits ordinarily imposed by the type and amount of basic data available, it is generally necessary to use approximate flood routing methods that either ignore some of the factors affecting flood wave movement or are based on simplifying assumptions in regard to such factors. Approximate methods produce results at considerably less expense but are limited in generality and accuracy which is the penalty one has to pay for their simplicity and low cost of usage.

Methods of flood routing are broadly classified as empirical, hydrological, simplified hydraulics and hydraulics. Empirical methods were generally developed from intuitive processes rather than from mathematical formulation of the problem. Their application is limited in practice for situations in which sufficient observations of inflows and outflows are available to calibrate the needed coefficients (Fread,1981).

Hydrological methods are based on some mathematical formulation of continuity equation in lumped form and, generally, a storage equation. The parameters involved in the mathematical formulation of the hydrological method are evaluated using past observations. Simplified hydraulic methods may use continuity equation either in lumped form (Hyami, 1951; Harley, 1967; Cunge, 1969 and Dooge et al., 1982) or in distributed form (Thomas and Wormleaton, 1970 and NERC, 1975) in addition to simplified form of the momentum equation of St. Venants' equations. The said simplification may be obtained either by curtailing certain terms based on the consideration of order of magnitude analysis of these terms with that of bed slope, S_o (Hyami, 1951; and Lighthill and Whitam, 1955) or by curtailing and replacing the terms by some appropriate approximation (Apollov et al.,1964).

It is possible to classify certain flood routing techniques under the category of both hydrological and simplified methods depending on the parameter estimation procedure. The typical example being the Muskingum method. The conventional Muskingum method introduced by McCarthy (1938) may be classified as a hydrological method wherein the parameters K and θ, respectively the travel time and the weighting coefficient are estimated based on the past observations. But the variations of the Muskingum method introduced by Cunge (1969), Dooge (1973), Koussis (1978) and Dooge et al.(1982) may fall under the category of simplified hydraulic method, wherein the parameters K and θ are related to the channel and flow

characteristics.

In practice hydrologic models are in vogue for many years. Well known among them are the Muskingum method (McCarthy, 1938), lag and route method (Meyer, 1941) and Nash Model (Dooge, 1973). These methods use the parameters calibrated from the past flood records for routing floods for the purpose of forecasting or simulation. Since the flood characteristics are likely to vary from one flood to another, it would be rash to assume that the parameters determined from one set of flood observations could be used to predict the behaviour of an altogether different flood. This, in effect, limits the predictive capability of the hydrological methods to floods similar to that used in the calibration, and any attempt at extrapolation is unwarrented. This necessitates the use of simplified hydraulic models in practice which enables one to determine the parameters in terms of physical system characteristics. Such methods enables either flood analyses to be performed in area where data are not available in sufficient quantity and/or quality or do not exist at all or for studying the future behaviour of the system subject to land use change including channel improvement. Well known examples of the simplified hydraulic models are the linear convection-diffusion method introduced by Hyami(1951), Kalinin-Milyukov method (Apollov et al.,1964), the complete linearized model (Harley, 1967), Muskingum-Cunge method (Cunge, 1969) etc.

The adoption of constant parameters simplified hydraulic models for routing a flood wave is based on the

assumption of linearity and this is in contradiction with the nonlinear property of flood waves. The wide use of constant parameter simplified hydraulic models such as Kalinin-Milyukov and Muskingum-Cunge methods in practice demonstrate that the accuracy of routing results is not severely affected. However, this aspect has not been conclusively proved. The constant parameters of these models are estimated based on the assumption that the flow variation takes place around a reference discharge. This limitation produces distortion in the predicted outflow when wide variation in the flow variable are considered. Keefer and McQuivey (1974) state that if the model is linearized about a high discharge, the low flows arrived too soon and are over damped and if it is linearized around a low discharge the peaks arrive late and are underdamped.

This has led to the development of variable parameter diffusion model (NERC,1975), variable parameter Muskingum-Cunge model (Ponce and Yevjevich, 1978), variable parameter Muskingum-Koussis model(Kousis,1978) etc. The most desirable way the nonlinearity in the flood routing process may be taken into account is to use such a model that remains linear at one time level, but the linear characteristics may change from one time level to another time level. Thus the parameters involved in the modelling vary from time to time just as the flow variable involved in the phenomena. This concept has been adopted by Ponce and Yevjevich (1978), and Koussis (1978) while they applied the Muskingum method based on

the diffusion analogy principle. Whereas Ponce and Yevjevich (1978) considered the variation of both K and θ, the travel time and weighting parameter respectively of the Muskingum method from one time step to another, Koussis considered the variation of K only keeping θ constant.

In an earlier report (Perumal, 1986-87), the author presented a variable parameter simplified hydraulic model for routing floods, without considering lateral inflow, in uniform rectangular channels having constant bed slope, by considering the variation of flow characteristics at each time level and by adopting linear solution approach.

In this report a variable parameter simplified hydraulic flood routing model without considering lateral inflow is developed for routing floods in uniform trapezoidal channels having constant bed slope, using the same solution approach as adopted in the earlier study. It is also shown that the solution equations developed for routing floods in uniform rectangular channel with constant bed slope is a particular case of the solution developed for trapezoidal channel. Also the inference arrived from this study regarding Muskingum method is same as inferred in the earlier study.

2.0 REVIEW

In this section, only those flood routing models which take into account the nonlinearity of the routing process by remaining in the linear solution domain at any time level, but varying the linear characteristics from one time level to another time level have been reviewed It is well known that the routing process is nonlinear in nature and therefore flood routing models with variable coefficients can be expected to perform better. It has been shown by Keefer and McQuivey (1974) that if the inflow hydrograph into a channel reach is considered in several blocks with each block having its own reference or linearizing discharge then the convolution of these inflow blocks with the corresponding unit hydrographs of the channel reach developed based on the reference discharge of each block yield routed hydrographs comparable well with the observed hydrograph than that routed hydrograph obtained based on the convolution of the inflow hydrograph with the unit hydrograph corresponding to a single reference discharge for the entire inflow hydrograph. This envisages the need for adopting variable parameter routing models.

Koussis (1978) developed a variable parameter Muskingum method based on the diffusion analogy principle, using the same concept as adopted by Cunge (1969), with constant weighting parameter θ and varying travel time K. Koussis (1978) has found from his experience that θ is not varying considerably with discharge, when compared with K. Koussis varied the

value of K at each time step by averaging the travel speed of the flood wave estimated at the upstream and downstream sections of the reach by introducing the correction in the rating curve at the respective sections using " Jones formula" (Henderson, 1966) as given below:

$$Q = Q_n\left(1 + \frac{1}{c\,So}\frac{\partial y}{\partial t}\right)^{\frac{1}{2}} \qquad \ldots(1)$$

in which,

Q = the discharge at a section during unsteady flow

Q_n = the normal discharge at the same section corresponding to the flow depth y observed during unsteady flow

c = the travel speed corresponding to discharge Q at a section

t = notation denoting time

By iteratively solving equation (1), the travel speeds at the upstream and downstream sections may be obtained corresponding to each time level of the Muskingum method solution. Koussis (1978) estimated the outflow discharge Q, using the following expression obtained by assuming linear variation of inflow over the routing time interval Δt:

$$Q_2 = C_1 I_2 + C_2 I_1 + C_3 Q_1 \qquad \ldots(2)$$

Wherein the coefficients C_1, C_2 and C_3 are given as:

$$C_1 = 1 - \frac{K}{\Delta t}(1 - \beta)$$

$$C_2 = \frac{K}{\Delta t}(1 - \beta) - \beta \quad \text{and} \qquad \ldots(3)$$

$$C_3 = \beta$$

Where $\beta = e^{-\Delta t/K(1-\theta)}$

Following the same approach of Cunge (1969), Koussis estimated the parameters θ and K in terms of Channel and flow characteristics by relating the numerical diffusion with the physical diffusion. The form of the parameters so estimated are given as:

$$\theta = 1 - \frac{\Delta t/K}{\ln\left(\frac{\lambda+1+\Delta t/K}{\lambda+1-\Delta t/K}\right)} \qquad \ldots(4)$$

Where

$$\lambda = \frac{Q_o}{BS_o c\ \Delta x}$$

Q_o = Reference discharge.

and

$$K = \Delta x/c \qquad \ldots(5)$$

The symbols B and Δx represents respectively, the channel width and reach length. The estimation of discharge at the outflow section requires one more iteration procedure using equation (2) besides the iteration required for the correction of rating curve at downstream section for the estimation of travel speed based on the loop rating curve. Therefore it can be realized that although the Koussis procedure is physically based, it involves tedious iterative computations.

Ponce and Yevjevich (1978) suggested a simple variable parameter method based on the Muskingum-Cunge procedure. Usually the routing time interval being fixed, and Δx and S_o are specified for each computational cell constituting of four

grid points, as shown in figure (1), their method involves the determination of flood wave celerity and the unit width discharge, q for each computational cell. The values of c and q at grid point (j,n) are defined by

$$c = \left.\frac{dQ}{dA}\right|_{j,n} \qquad \ldots(6)$$

$$q = \left.\frac{Q}{B}\right|_{j,n} \qquad \ldots(7)$$

in which

Q = discharge

A = flow area

The following ways of determining c and q were investigated by Ponce and Yevjevich for the computation of variables θ and K of Cunge (1969) for each time level:

(1) directly by using a two point average of the values at grid points (j,n) and (j+1,n);

(2) directly by using a three point average of the values at grid points (j,n), (j+1,n) and (J,n+1); and

(3) by iteration, using a four point average calculation.

They concluded that three point and four point iterative schemes of varying c and q yield better results and both are comparable. In view of iterations involved in four point scheme,it may be considered that three point average procedure is desirable for use in practice. Besides, this method is also much simpler than the method suggeted by Koussis (1978). However both Ponce and Yevjevich's (1978), and Koussis '(1978) approaches for varying the parameters of

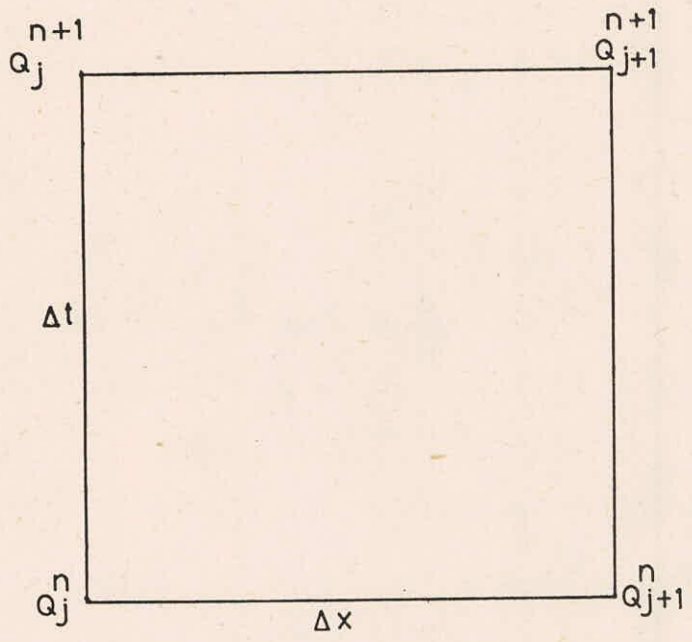

FIG.1. SPACE TIME DISCRETIZATION OF MUSKINGUM METHOD

the Muskingum method at each routing time level are arbitrary and not based on the mathematics of the Muskingum method solution.

In an earlier study(Perumal, 1986-87) the author presented a variable parameter simplified hydraulic method based on the approximation of the St. Venant s equations for routing floods, without considering lateral inflow, in channels having uniform rectangular cross-section and constant bed slope. The method was developed assuming that the friction slope S_f is constant at any instant of time over the channel routing reach and by adopting the concept that during unsteady flow there exists a one to one relationship, at any instant of time, between the stage at the middle of the routing reach and the discharge downstream of it. The form of the governing equation for obtaining the solution is same as that Muskingum method which is given as:

$$I - Q = \frac{d}{dt} K[Q + \theta (I-Q)] \qquad ...(8)$$

in which

$$K = \frac{\Delta x}{[\frac{5}{3} - \frac{4}{3} (\frac{y_3}{B + 2y_3})] v_3} \qquad ...(9)$$

and

$$\theta = \frac{1}{2} - Q_n[\frac{1}{2} - \frac{\frac{1}{2}(\frac{1}{2}-1)}{\lfloor 2} G_m + \frac{\frac{1}{2}(\frac{1}{2}-1)(\frac{1}{2}-2)}{\lfloor 3} G_m^2$$

$$+ .....] \frac{1-\frac{4}{9} F^2(1- \frac{2y_m}{B+2y_m})^2}{S_o B[\frac{5}{3} - \frac{4}{3} (\frac{y_m}{B + 2y_m})] v_m \quad \Delta x} \qquad ...(10)$$

where,

$$G_m = \frac{1 - \frac{4}{9}F^2 \left(1 - \frac{2y_m}{B+2y_m}\right)^2}{S_o B \left[\frac{5}{3} - \frac{4}{3}\frac{y_m}{(B+2y_m)}\right] V_m} \frac{\partial Q}{\partial x} \quad \ldots(11)$$

The symbols y_3 ,v_3 and Q_3 respectively denote the flow depth, velocity and discharge at section downstream of the mid-section of the reach where the discharge during unsteady flow is uniquely related with the flow depth at mid-section of the reach, and y_m and v_m represent the flow depth and velocity at mid-section of the reach during unsteady flow. F is the Froude number corresponding to flow at the mid-section of the reach. For wide rectangular channels equations (9) and (10) reduce to

$$K = \frac{\Delta x}{\frac{5}{3} v_3} \quad \ldots(12)$$

and

$$\theta = \frac{1}{2} - Q_n \frac{\left[\frac{1}{2} - \frac{\frac{1}{2}(\frac{1}{2}-1)}{\lfloor 2} G_m + \frac{\frac{1}{2}(\frac{1}{2}-1)(\frac{1}{2}-2)}{\lfloor 3} G_m^2 + \ldots\right](1-\frac{4}{9}F^2)}{S_o B \left(\frac{5}{3} v_m\right) \Delta x} \quad \ldots(13)$$

when neglecting the terms G_m, G_m^2 , ...etc., θ reduces to

$$\theta = \tfrac{1}{2} - \frac{Q_n (1 - \frac{4}{9} F^2)}{2 S_o B \left(\frac{5}{3} v_m\right) \Delta x} \quad \ldots(14)$$

It was shown that when the variables are fixed corresponding to a reference discharge value Q_o,

$$K = \frac{\Delta x}{\frac{5}{3} v_o} \quad \ldots(15)$$

$$\theta = \tfrac{1}{2} - \frac{Q_o\,(1 - \frac{4}{9} F_o^2)}{2S_o B(\frac{5}{3} v_o)\,\Delta x} \qquad \ldots(16)$$

The above expression for K and θ were obtained by Dooge et. al. (1982) based on linearized St. Venant's solution approach, for the case of constant parameters Muskingum flood routing method. When the rectangular channel is not wide and after eliminating G_m , G_m^2 , ... etc. K and θ reduce to:

$$K = \frac{\Delta x}{[\frac{5}{3} - \frac{4}{3}\,(\frac{y_3}{B + 2y_3})]v_3} \qquad \ldots(17)$$

$$\theta = \tfrac{1}{2} - \frac{y_m Q_n [1 - \frac{4}{9} F^2 (1 - \frac{2y_m}{B + 2y_m})^2]}{2S_o\,[\frac{5}{3} - \frac{4}{3}\,(\frac{y_m}{B + 2y_m})]Q_m \Delta x} \qquad \ldots(18)$$

The developed method employed equation (17) and (18) for routing floods in four different channels having prismatic ractangular cross-section with different constant bed slopes and Manning's roughness coefficients, and the results were compared with the corresponding st. Venant's solutions. Three different solution approaches were used for routing floods in each channel corresponding to a reach length of 40 Km. These approaches consist of considering the entire 40 km. length as a single reach and obtaining the solution by varying θ and K; considering the entire 40 Km length as a single reach but obtaining the solution by varying K and keeping θ constant;

and considering the 40 km. reach consists of 8 equal sub-reaches and obtaining the solution by successively routing through these reaches by varying both θ and K. It was found that the last solution approach was able to reproduce more closely the St. Venant's solution of both stage and discharge hydrographs when compared with the other two approaches.

The study also brought out the theoretical reason for the reduced outflow in the beginning of the Muskingum solution and suggested the needed remedial measure to avoid it. Also it was shown using the developed theory that for Muskingum method the maximum value of θ is 0.5 and its negative value is admissible.

3.0 PROBLEM DEFINITION

It is required to develop a simplified hydraulic flood routing method for tracking flood wave movement in prismatic channels having uniform trapezoidal cross section and constant bed slope. The routing procedure may adopt a linear form of solution equation with the relevant parameters varying from one time level to another time level of solution and thus taking care of approximately the non-linear behaviour of the flood wave movement.

4.0 METHODOLOGY

The method developed herein is similar to that developed in the earlier study(Perumal, 1986-87) by the author for routing floods in uniform rectangular channels having constant bed slope and roughness coefficient. For the purpose of better understanding of the method developed herein, the physical basis of the proposed theory and the assumptions involved in the development of the method are once again described without referring it to the report quoted above.

4.1 Physical Basis of the Proposed Theory

During steady flow in a river reach there exists a unique relationship between stage and discharge at any cross section. This situation is altered during unsteady flow, with the discharge appearing first in a cross-section and at the same time the stage which corresponds to that discharge during steady flow appears at a section upstream of it. This concept has been adopted by Kalinin and Milyukov (as quoted by Miller and Cunge, 1975) to determine the 'unit length of reach' required for flood routing in river reaches. However, Kalinin-Milyukov method is less flexible since the 'unit reach length' of the channel is fixed for a given flood wave and the end section of the unit reach length may not coincide with the downstream section where the stage-discharge information is required, thus necessitating interpolation of the routed hydrographs. Besides, the adoption of constant unit reach length implies that the unique relationship between discharge at the outflow section and the depth at the middle of the reach

always exists during unsteady flow phenomena. This is in contradiction to the characteristics of unsteady flow phenomena in channels. In this report, it is shown that the modification of the concept of Kalinin-Milyukov method leads to a flood routing method which is devoid of such limitations mentioned above.

The concept adopted in the Kalinin-Milyukov method is that during unsteady flow in a uniform rectangular channel with linearly varying water stage along the river reach, the channel storage S in the routing reach of length Δx is uniquely related to the mean water stage of the reach which in turn is uniquely related with the discharge observed at the outlet of the reach. Here the distance Δx corresponds to the unit reach length.

The constant parameters of the Muskingum method have been evaluated by extending this concept that the mean water stage of the routing reach of length Δx is uniquely related to the discharge at a section located 'ℓ' units of length downstream of the midsection of the reach (Apollov et al, 1964). However, here Δx need not correspond to the unit reach length as in the case of Kalinin-Milyukov method.

The above concept has been used to evaluate the variable parameters of the proposed method. The mathematical description of the method which is different from that of Kalinin-Milyukov method is given in the following pages with the assumptions involved.

4.2 Assumptions

The following assumptions have been made in developing this method:

1. The channel reach is having uniform trapezoidal cross section.
2. The channel bottom slope is constant over the routing reach length.
3. There is no lateral inflow or outflow from the reach.
4. The friction slope S_f is constant at any instant of time over the channel routing reach.
5. During unsteady flow, there exists a one-to-one relationship at any instant of time between the stage at the middle of the routing reach and the discharge passing through a section downstream of it.

4.3 Development of the Model

Figure (2) depicts a river reach having uniform trapezoidal cross-section with upstream and downstream sections, where the inflow and outflow hydrographs are observed have been denoted respectively as sections (1) and (2). Let the distance between these sections be Δx. Let the side slope of the trapezoidal section be Z (Z Horizontal:1 vertical). The definition sketch of the trapezoidal section is also shown in fig.2.

Based on assumption (5), the water depth observed at the middle of the reach corresponds to the normal depth of that discharge which is observed, at the same instant of time, 'ℓ' units of distance downstream from the middle of the reach. Let

SECTION ①-① : CORRESPONDS TO THE INFLOW POINT

SECTION ②-② : CORRESPONDS TO THE OUTFLOW POINT

SECTION ③-③ : CORRESPONDS TO THE POINT WHERE THE DISCHARGE Q_e IS UNIQUELY RELATED WITH THE STAGE AT THE MIDSECTION OF THE REACH

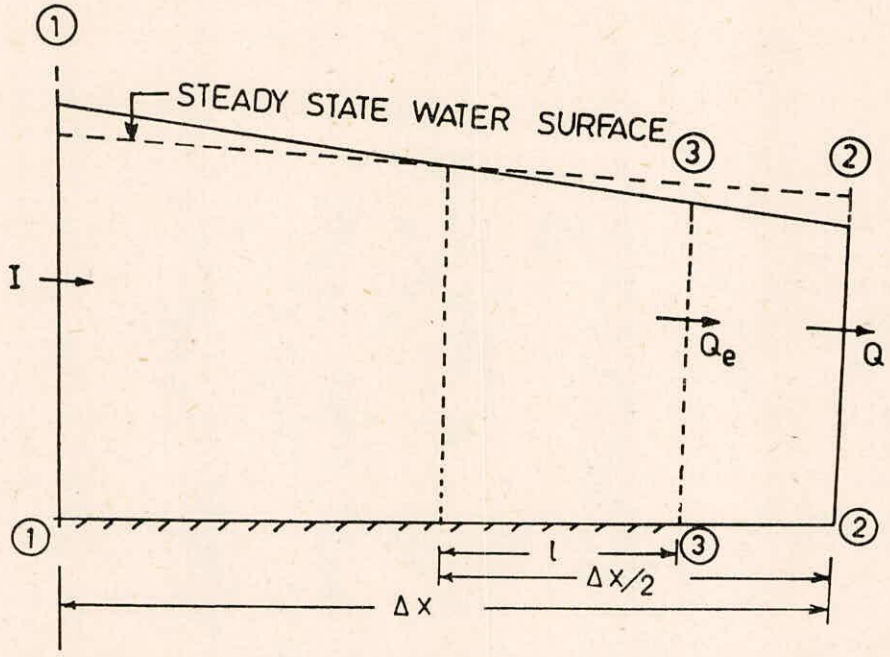

FIG. 2(a) DEFINITION SKETCH OF THE REACH UNDER CONSIDERATION

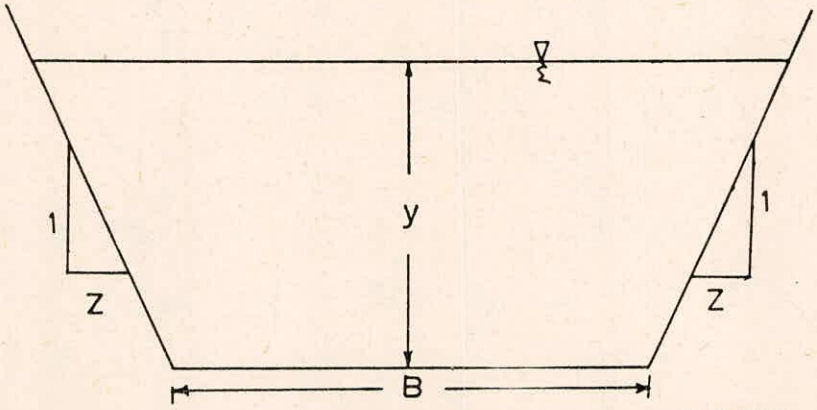

FIG. 2(b) DEFINITION SKETCH OF THE CROSS-SECTION OF THE REACH UNDER CONSIDERATION

this discharge be denoted as Q_n and the section where this discharge is observed be marked as section (3). The discharge at the middle of the reach may be expressed as:

$$Q_m = A_m v_m \tag{19}$$

where, A_m and v_m are the area and velocity during unsteady flow at this section. Equation (19) may be re-written in terms of width and side slope of channel section, depth of flow at the mid-section and Chezy's or Mannings roughness coefficient. First the mathematical formulation of the problem in terms of Chezy's friction law is presented followed by the formulation using Manning's friction law.

4.3.1 Mathematical formulation involving Chezy's law

Before proceeding with further mathematical operation on equation (19) using assumption (5), it is necessary to use assumption (4) in order to simplify the expression for friction slope which would be used in modifying equation (19).

Let the expression for discharge Q at any section of the reach during unsteady flow condition in the reach, as depicted by figure (2), may be expressed as:

$$Q = Av \tag{20}$$

where, A is the channel cross section and v is the velocity of flow. The discharge using Chezy's friction law is given as:

$$Q = AC\sqrt{RS_f} \tag{21}$$

where

C = Chezy's constant

R = A/P, the hydraulic radius

P = the wetted perimeter, and

S_f = the friction slope

The area of cross section of the trapezoidal section is expressed as:

$$A = (B + yZ)y \qquad \ldots(22)$$

where

B = the bottom width, and

Z = the side slope (Z horizontal : 1 vertical)

The wetted perimeter of the trapezoidal section is expressed as:

$$P = (B + 2y\sqrt{1 + Z^2}) \qquad \ldots(23)$$

The hydraulic radius of the trapezoidal section is expressed as:

$$R = (B + yZ)y/(B + 2y\sqrt{1 + Z^2}) \qquad \ldots(24)$$

Equation (21) is re-written in terms of channel width, side slope and depth of flow as:

$$Q = \frac{C[(B + yZ)y]^{3/2} S_f^{\frac{1}{2}}}{[B + 2y\sqrt{1+Z^2}]^{\frac{1}{2}}} \qquad \ldots(25)$$

The friction slope S_f can be expressed as (Henderson, 1966):

$$S_f = S_o - \frac{\partial y}{\partial x} - \frac{v}{g}\frac{\partial v}{\partial x} - \frac{1}{g}\frac{\partial v}{\partial t} \qquad \ldots(26)$$

Where,

S_o = the bed slope

$\frac{\partial y}{\partial x}$ = the water surface slope

$\frac{V}{g}\frac{\partial v}{\partial x}$ = convective acceleration slope

$\frac{1}{g}\frac{\partial v}{\partial t}$ = local acceleration slope

x = notation denoting distance

g = the acceleration due to gravity(9.81 m/sec^2).

Differentiating Q as given by equation (21) w.r.t. x:

$$\frac{\partial Q}{\partial x} = C\sqrt{S_f}\,\frac{\partial}{\partial x}(A\sqrt{R}) + CA\sqrt{R}\,\frac{\partial}{\partial x}(S_f^{\frac{1}{2}}) \qquad \ldots(27)$$

Based on assumption (4) that S_f remains constant at any instant of time, the above equation reduces to:

$$\frac{\partial Q}{\partial x} = C\sqrt{S_f}\,\frac{\partial}{\partial x}(A\sqrt{R}) \qquad \ldots(28)$$

On further manipulation the above equation reduces as:

$$\frac{\partial Q}{\partial x} = v\left[\frac{P}{2}\cdot\frac{\partial R}{\partial x} + \frac{\partial A}{\partial x}\right] \qquad \ldots(29)$$

The differential $\frac{\partial R}{\partial x}$ can be expressed as:

$$\frac{\partial R}{\partial x} = \frac{(B+2YZ)}{(B+2y\sqrt{1+z^2})}\,\frac{\partial y}{\partial x} - \frac{2(B+yZ)\,y\,\sqrt{1+Z^2}}{(B+2y\sqrt{1+Z^2})}\,\frac{\partial y}{\partial x} \qquad \ldots(30)$$

The differential $\frac{\partial A}{\partial x}$ can be expressed as

$$\frac{\partial A}{\partial x} = (B + 2yZ)\,\frac{\partial y}{\partial x} \qquad \ldots(31)$$

Substituting eqns. (30) and (31) in eqn.(29) yields

$$\frac{\partial Q}{\partial x} = v \left[\frac{3}{2}(B + 2YZ) - \frac{(B+yZ)y\sqrt{1+Z^2}}{(B+2y\sqrt{1+Z^2})} \right] \frac{\partial y}{\partial x} \qquad \ldots(32)$$

The above equation can also be expressed as

$$\frac{\partial Q}{\partial x} = v \left[\frac{3}{2}\frac{\partial A}{\partial y} - R\sqrt{1+Z^2} \right] \frac{\partial y}{\partial x} \qquad \ldots(33)$$

When S_f remains constant at any instant of time over the reach under consideration, the terms $\frac{v}{g}\frac{\partial v}{\partial x}$, $\frac{1}{g}\frac{\partial v}{\partial t}$ and $\frac{\partial y}{\partial x}$ of eqn. (26) also remains constant. This implies during unsteady flow, the water surface is linearly varying at any instant of time over the routing reach.

Defferentiating eqn. (32) yields:

$$\frac{\partial^2 Q}{\partial x^2} = v\left[\frac{3}{2}\frac{\partial}{\partial x}(B+2YZ) - \frac{\partial}{\partial x}\frac{(B+yZ)y\sqrt{1+Z^2}}{(B+2y\sqrt{1+Z^2})} \right] \frac{\partial y}{\partial x}$$

$$+v\left[\frac{3}{2}(B+2yZ) - \frac{(B+yZ)y\sqrt{1+Z^2}}{(B+2y\sqrt{1+Z^2}} \right] \frac{\partial^2 y}{\partial x^2}$$

$$+ \left[\frac{3}{2}(B+2yZ) - \frac{(B+yZ)y\sqrt{1+Z^2}}{(B+2y\sqrt{1+Z^2}} \right] \frac{\partial v}{\partial x}\frac{\partial y}{\partial x} \qquad \ldots(34)$$

Assuming the terms $\frac{\partial^2 y}{\partial x^2}$, $(\frac{\partial y}{\partial x})^2$ and $\frac{\partial v}{\partial x}\cdot\frac{\partial y}{\partial x}$ are negligible in magnitude when compared with the magnitude of $\frac{\partial y}{\partial x}$, eqn. (34) can be approximated to :

$$\frac{\partial^2 Q}{\partial x^2} = 0 \qquad \ldots(35)$$

Eqn.(35) implies that Q is also varying linearly over

the reach where S_f is considered constant, at any instant of time.

Evaluation of terms $\frac{v}{g}\frac{\partial v}{\partial x}$ and $\frac{1}{g}\frac{\partial v}{\partial t}$ in terms of $\frac{\partial y}{\partial x}$:-

Using equation (20) and (33) one can arrive at the expression for $\frac{v}{g}\frac{\partial v}{\partial x}$ at any section in the reach in terms of hydraulic radius, top width of flow section and Froude number as:

$$\frac{v}{g}\frac{\partial v}{\partial x} = \left[\frac{1}{2} - \frac{R\sqrt{1+Z^2}}{\partial A/\partial y}\right] F^2 \frac{\partial y}{\partial x} \qquad \ldots(36)$$

Similarly using the hydraulic continuity equation which is given as :

$$\frac{\partial Q}{\partial x} + \frac{\partial A}{\partial t} = 0 \qquad \ldots(37)$$

and eqns. (20) and (33), the expressioin for $\frac{1}{g}\frac{\partial v}{\partial t}$ at any section of the reach is given as:

$$\frac{1}{g}\frac{\partial v}{\partial t} = F^2\left[-\frac{3}{4} + 2\frac{R\sqrt{1+Z^2}}{\frac{\partial A}{\partial Y}} - \left(\frac{R}{\frac{\partial A}{\partial y}}\right)^2 (1+Z^2)\right]\frac{\partial y}{\partial x} \qquad \ldots(39)$$

Therefore the friction slope expressed by equation (26) can be modified for the routing reach under consideration, using equations(39) and (36) as:

$$S_f = S_o\left(1-\frac{1}{So}\frac{\partial y}{\partial x}\left[1-\frac{F^2}{4}\left(1-2\frac{R}{\frac{\partial A}{\partial y}}\sqrt{1+Z^2}\right)^2\right]\right) \qquad \ldots(40)$$

The discharge at the middle of the reach is expressed as:

$$Q_m = A_m v_m \qquad \ldots(19)$$

Equation (19) is re-written in terms of area and wetted perimeter as:

$$Q_m = A_m C\sqrt{\frac{A_m}{P_m} S_f} \qquad \ldots(41)$$

Where P_m is the wetted perimeter at the mid-section of the reach and other symbols are as defined earlier. Q_m may be re written after substituting for S_f from equation (40) into equation (41) as:

$$Q_m = A_m C\sqrt{\frac{A_m}{P_m} S_o} \left\{1-\frac{1}{S_o}\frac{\partial y}{\partial x}\Big|_m \left[1-\frac{F^2}{4}\left(1-2\frac{R_m}{\frac{\partial A}{\partial y}\Big|_m}\sqrt{1+Z^2}\right)^2\right]\right\}^{\frac{1}{2}} \quad \ldots(42)$$

where

R_m = the hydraulic radius at mid section of the reach

$\frac{\partial y}{\partial x}|_m$ = the water surface slope at the mid-section of the reach

$\frac{\partial A}{\partial y}|_m$ = the top width of flow section at the middle of the reach

Based on assumption (5), the flow depth observed at the mid section of the reach corresponds to the normal depth of discharge Q_n which is occuring somewhere downstream of the mid-section of the reach. Therefore the term $A_m C\sqrt{\frac{A_m}{P_m} S_o}$ corresponds to the discharge Q_n

Thus equation (42) is modified as:

$$Q_m = Q_n \left[1-\frac{1}{S_o}\frac{\partial y}{\partial x}\Big|_m \left(1-\frac{F^2}{4}\left(1-2\frac{R_m}{\frac{\partial A}{\partial y}\Big|_m}\sqrt{1+Z^2}\right)^2\right)\right]^{\frac{1}{2}} \quad \ldots(43)$$

Based on the typical value of S_o, $\frac{\partial y}{\partial x}$ experienced in natural rivers (Henderson, 1966) it may be considered that the absolute value of the term

$$\frac{1}{S_o}\frac{\partial y}{\partial x}\Big|_m \left[1-\frac{F^2}{4}\left(1-2\frac{R_m}{\frac{\partial A}{\partial y}\Big|_m}\sqrt{1+Z^2}\right)^2\right] < 1$$

Under such situation the Binomial series expansion of eqn.(43)

is convergent, and it is given as :

$$Q_m = Q_n \{ 1 - \frac{1}{2S_o}\frac{\partial y}{\partial x}|_m [1 - \frac{F^2}{4}(1 - \frac{2R_m}{\frac{\partial A}{\partial y}|_m}\sqrt{1+Z^2})^2]$$

$$+ \frac{\frac{1}{2}(\frac{1}{2}-1)}{\lfloor 2} [\frac{1}{S_o}\frac{\partial y}{\partial x}|_m (1-\frac{F^2}{4}\{1-2\frac{R_m}{\frac{\partial A}{\partial y}|_m}\sqrt{1+Z^2})^2\}]^2$$

$$- \frac{\frac{1}{2}(\frac{1}{2}-1)(\frac{1}{2}-2)}{\lfloor 3} [\frac{1}{S_o}\frac{\partial y}{\partial x}|_m (1-\frac{F^2}{4}\{1-2\frac{R_m}{\frac{\partial A}{\partial y}|_m}\sqrt{1+Z^2})^2\}]^3$$

$$+ \ldots\ldots\ldots \} \qquad \ldots(44)$$

Let the term $\frac{1}{So}\frac{\partial y}{\partial x}|_m [1-\frac{F^2}{4}(1-2\frac{R_m}{\frac{\partial A}{\partial y}|_m}\sqrt{1+Z^2})^2] = G \qquad \ldots(45)$

Eqn. (44) is written in terms of G as

$$Q_m = Q_n - Q_n[\frac{1}{2} + \frac{1}{8}G + \frac{1}{16}G^2 + \frac{5}{128}G^3 + \ldots.]$$

$$\frac{[1 - \frac{F^2}{4}(1-2\frac{R_m}{\frac{\partial A}{\partial y}|_m}\sqrt{1+Z^2})^2]\frac{\partial y}{\partial x}|_m}{S_o} \qquad \ldots(46)$$

Eqn. (46) is modified by replacing $\frac{\partial y}{\partial x}$ by $\frac{\partial Q}{\partial x}$ using eqn. (33) as:

$$Q_m = Q_n - Q_n [\frac{1}{2} + \frac{1}{8}G + \frac{1}{16}G^2 + \frac{5}{128}G^3 \ldots.]$$

$$\frac{[1 - \frac{F^2}{4}(1-2\frac{R_m}{\frac{\partial A}{\partial y}|_m}\sqrt{1+Z^2})^2]}{v_m S_o[\frac{3}{2}\frac{\partial A}{\partial y}|_m - R_m\sqrt{1+Z^2}]}\frac{\partial Q}{\partial x}|_m \qquad \ldots(47)$$

Since the discharge is varying linearly $\frac{\partial Q}{\partial x}|_m = \frac{\partial Q}{\partial x}|_3 \qquad \ldots(48)$

where,

$\frac{\partial Q}{\partial x}|_3$ = the rate of change of discharge at section (3)

Therefore eqn. (47) is modified as:

$$Q_m = Q_n - Q_n \left[\tfrac{1}{2} + \frac{1}{8}G + \frac{1}{16}G^2 + \frac{5}{128}G^3 + \ldots\ldots\right]$$

$$\frac{\left[1 - \frac{F^2}{4}\left(1-2\,\frac{R_m}{\frac{\partial A}{\partial y}|_m}\sqrt{1+z^2}\right)^2\right]}{v_m S_o \frac{\partial A}{\partial y}|_m \left[\frac{3}{2} - \frac{Rm}{\frac{\partial A}{\partial y}|_m}\sqrt{1+Z^2}\right]} \frac{\partial Q}{\partial x}|_3 \qquad \ldots(49)$$

Therefore the distance 'ℓ' between the mid-section and that downstream section at which the normal discharge corresponding to the depth observed at mid section is given as:

$$\ell = Q_n\left[\tfrac{1}{2} + \frac{1}{8}G + \frac{1}{16}G^2 + \frac{5}{128}G^3 + \ldots\ldots\right]$$

$$\frac{\left[1 - \frac{F^2}{4}\left(1-2\,\frac{R_m}{\frac{\partial A}{\partial y}|_m}\sqrt{1+Z^2}\right)^2\right]}{v_m S_o \frac{\partial A}{\partial y}|_m \left[\frac{3}{2} - \frac{R_m}{\frac{\partial A}{\partial y}|_m}\sqrt{1+Z^2}\right]} \qquad \ldots(50)$$

Since the discharge is varying linearly within the reach of length Δx, the discharge Q_n at section (3) is computed in terms of inflow I and outflow Q as:

$$Q_n = Q + \left(\tfrac{1}{2} - \frac{\ell}{\Delta x}\right)(I - Q) \qquad \ldots(51)$$

Now applying the continuity equation

$$\frac{\partial Q}{\partial x} + \frac{\partial A}{\partial t} = 0 \qquad \ldots(37)$$

between sections (1) and (3) of figure (2), one arrives at

$$\frac{\partial Q}{\partial x}\Big|_3 = -\frac{1}{\frac{\partial Q}{\partial A}\Big|_3} \quad \frac{\partial Q}{\partial t}\Big|_3 \qquad \ldots(52)$$

But using equation (33), $\frac{\partial Q}{\partial A}$ may be written as:

$$\frac{\partial Q}{\partial A}\Big|_3 = v_3 \left[\frac{3}{2} - \frac{R_3}{\frac{\partial A}{\partial y}\Big|_3} \sqrt{1+Z^2} \right] \qquad \ldots(53)$$

where,

v_3 = velocity of flow at section (3)

Therefore substituting eqn. (53) in eqn. (52) yields:

$$\frac{\partial Q}{\partial x}\Big|_3 = - \frac{1}{v_3\left[\frac{3}{2} - \frac{R_3}{\frac{\partial A}{\partial y}\Big|_3} \sqrt{1+Z^2}\right]} \frac{\partial}{\partial t}(Q_3) \qquad \ldots(54)$$

Since $\frac{\partial Q}{\partial x}\Big|_3 = \frac{\partial Q}{\partial x}\Big|_2$ as inferred from eqn. (35), eqn(54) is modified and written in numerical difference form as

$$I - Q = \frac{\Delta x}{v_3\left[\frac{3}{2} - \frac{R_3}{\frac{\partial A}{\partial y}\Big|_3} \sqrt{1+Z^2}\right]} \frac{\partial}{\partial t}(Q_3) \qquad \ldots(55)$$

But Q_3 is same as Q_n and it is given by eqn. (51)

Therefore Eqn.(55) is modified as:

$$I - Q = \frac{\Delta x}{v_3\left[\frac{3}{2} - \frac{R_3}{\frac{\partial A}{\partial y}\Big|_3} \sqrt{1+z^2}\right]} \cdot \frac{\partial}{\partial t}\left[Q + \left(\tfrac{1}{2} - \frac{\ell}{\Delta x}\right)(I-Q)\right] \qquad \ldots(56)$$

Since I and Q varies only w.r.t. t, the partial derivative of eqn.(56) is changed to full derivative and the eqn.(56) is modified as:

$$I - Q = \frac{d}{dt} K \left[Q + \left(\tfrac{1}{2} - \frac{\ell}{\Delta x}\right) (I - Q) \right] \qquad \ldots(57)$$

where,

ℓ is given by eqn. (50) and

$$K = \frac{\Delta x}{v_3 \left[\frac{3}{2} - \frac{R_3}{\frac{\partial A}{\partial y}\Big|_3} \sqrt{1+Z^2} \right]} \qquad \ldots(58)$$

Eqn(57) is of the same form as that of well known Muskingum method.

Parameter θ is approximated by neglecting the terms G, G^2, G^3... in eqn. (50) as:

$$\theta = \tfrac{1}{2} - \frac{Q_n \left[1 - \frac{F^2}{4}\left(1 - 2 \frac{R_m}{\frac{\partial A}{\partial y}\Big|_m} \sqrt{1+Z^2}\right)^2 \right]}{2 S_o v_m \frac{\partial A}{\partial y}\Big|_m \left[\frac{3}{2} - \frac{R_m}{\frac{\partial A}{\partial y}\Big|_m} \sqrt{1+Z^2}\right] \Delta x} \qquad \ldots(59)$$

Eqn.(59) is more suitable for use in practice:

Expressing equations (58) and (59) in terms of channel width and flow depth as:

$$K = \frac{\Delta x}{v_3 \left[\frac{3}{2} - \frac{(B+y_3 Z)\, y_3 \sqrt{1+Z^2}}{(B+2y_3\sqrt{1+Z^2})\,(B+2y_3 Z)} \right]} \qquad \ldots(60)$$

where,

y_3 = flow depth at section (3), and

$$\theta = \tfrac{1}{2} - \frac{Q_3 \left[1 - \frac{F^2}{4}\left(1 - \frac{2(B + Zy_m) y_m \sqrt{1+Z^2}}{(B + 2y_m\sqrt{1+Z^2})(B+2y_m Z)}\right)^2 \right]}{2S_o v_m (B+2y_m Z)\left[\frac{3}{2} - \frac{(B+y_m Z) y_m \sqrt{1+Z^2}}{(B+2y_m\sqrt{1+Z^2})(B+2y_m Z)} \right] \Delta x} \qquad \ldots(61)$$

when the flow variables are fixed at reference values, then K and θ reduce to

$$K = \frac{\Delta x}{v_o\left[\frac{3}{2} - \frac{(B+y_oZ)\, y_o\sqrt{1+Z^2}}{(B+2y_o\sqrt{1+Z^2})(B+2y_oZ)}\right]} \qquad \ldots(62)$$

and

$$\theta = 1/2 - \frac{Q_o\left[1-\frac{F_o^2}{4}\left(1-\frac{2(B+y_oZ)y_o\sqrt{1+Z^2}}{(B+2y_o\sqrt{1+Z^2})(B+2y_oZ)}\right)^2\right]}{2\,S_o v_o(B+2y_oZ)\left[\frac{3}{2}-\frac{(B+y_oZ)y_o\sqrt{1+Z^2}}{(B+2y_o\sqrt{1+Z^2})(B+2y_oZ)}\right]\Delta x} \qquad \ldots(63)$$

Reducing K and θ for rectangular cross-section channel case:

For rectangular cross section Z = 0.

When Z = 0, equations (60) and (61) reduce to:

$$K = \frac{\Delta x}{v_3\left[\frac{3}{2} - \frac{y_3}{B+2y_3}\right]} \qquad \ldots(64)$$

and

$$\theta = \tfrac{1}{2} - \frac{Q_3\left[1-\frac{F^2}{4}\left(\frac{B}{B+2y_m}\right)^2\right]}{2BS_o v_m\left(\frac{3}{2} - \frac{y_m}{B+2y_m}\right)\Delta x} \qquad \ldots(65)$$

4.3.2 Mathematical formulation involving Manning's friction law:

Proceeding in the similar manner as in the case of analyis based on Chezy's friction law, the expression for $\frac{\partial Q}{\partial x}$ using Manning's friction law is given as:

$$\frac{\partial Q}{\partial x} = v\left[\frac{5}{3}(B+2yZ) - \frac{4}{3}\,\frac{(B+yZ)y\sqrt{1+Z^2}}{(B+2y\sqrt{1+Z^2})}\right]\frac{\partial y}{\partial x} \qquad \ldots(66)$$

The equation can also be expressed as:

$$\frac{\partial Q}{\partial x} = v\left[\frac{5}{3}\frac{\partial A}{\partial y} - \frac{4}{3}R\sqrt{1+Z^2}\right]\frac{\partial y}{\partial x} \qquad \ldots(67)$$

It can be proved, as it has been done earlier for the unsteady flow governed by Chezy's law, that $\frac{\partial Q}{\partial x}$ is also varying linearly at any routing time level over the reach where the friction slope S_f is assumed constant.

Evaluation of the terms $\frac{v}{g}\frac{\partial v}{\partial x}$ and $\frac{1}{g}\frac{\partial v}{\partial t}$ in terms of $\frac{\partial y}{\partial x}$:

Using equations (20) and (67), the expression for $\frac{v}{g}\frac{\partial v}{\partial x}$ at any section in the reach is given in terms of hydraulic radius, top width of flow section and Froude number as:

$$\frac{v}{g}\frac{\partial v}{\partial x} = \left[\frac{2}{3} - \frac{4}{3}\frac{R}{\frac{\partial A}{\partial y}}\sqrt{1+Z^2}\right] F^2 \frac{\partial y}{\partial x} \qquad \ldots(68)$$

where,

F denotes the Froude number of flow.

Similarly the expression for $\frac{1}{g}\frac{\partial v}{\partial t}$ at any section of the reach is given as:

$$\frac{1}{g}\frac{\partial v}{\partial t} = \left[-\frac{10}{9} + \frac{28}{9}\frac{R}{\frac{\partial A}{\partial y}}\sqrt{1+Z^2} - \frac{16}{9}\left(\frac{\frac{R^2}{\partial A}}{\partial y}\right)^2(1+Z^2)\right]F^2 \frac{\partial y}{\partial x} \qquad \ldots(69)$$

The addition of equations (68) and (69) yield:

$$\frac{v}{g}\frac{\partial v}{\partial x} + \frac{1}{g}\frac{\partial v}{\partial t} = -\frac{4}{9}F^2\left(1 - \frac{2R\sqrt{1+Z^2}}{\frac{\partial A}{\partial y}}\right)^2 \frac{\partial y}{\partial x} \qquad \ldots(70)$$

Therefore the friction slope expressed by equation (26) can be modified for the routing reach under consideration as:

$$S_f = S_o\left\{1 - \frac{1}{S_o}\frac{\partial y}{\partial x}\left[1 - \frac{4}{9}F^2\left(1 - \frac{2R}{\frac{\partial A}{\partial y}}\sqrt{1+Z^2}\right)^2\right]\right\} \qquad \ldots(71)$$

Based on similar analysis as carried out for the case of unsteady flow following chezy's friction law, it can be shown that the distance 'ℓ' between the mid-section and that

downstream section at which the normal discharge corresponding to the flow depth of mid-section is experienced, is given as

$$\ell = Q_n\left[\tfrac{1}{2} + \frac{1}{8}G_m + \frac{1}{16}G_m + \frac{5}{128}G_m^3 + \ldots.\right] \frac{\left[1 - \frac{4}{9}F^2\left(1-2\frac{R_m}{\frac{\partial A}{\partial y}\big|_m}\sqrt{1+Z^2}\right)^2\right]}{v_m S_o \frac{\partial A}{\partial y}\big|_m\left[\frac{5}{3} - \frac{4}{3}\frac{R_m}{\frac{\partial A}{\partial y}\big|_m}\sqrt{1+Z^2}\right]} \qquad \ldots(72)$$

where,

$$G_m = \frac{1-\frac{4}{9}F^2\left(1 - 2\frac{R_m}{\frac{\partial A}{\partial y}\big|_m}\sqrt{1+Z^2}\right)^2}{v_m S_o \frac{\partial A}{\partial y}\big|_m\left[\frac{5}{3} - \frac{4}{3}\frac{R_m}{\frac{\partial A}{\partial y}\big|_m}\sqrt{1+Z^2}\right]} \cdot \frac{\partial Q}{\partial x}\Big|_m \qquad \ldots(73)$$

and $R_m \cdot \frac{\partial A}{\partial y}\big|_m$, v_m are as defined earlier for the derivation using Chezy's friction law.

Similar analysis as carried out earlier for the flow following Chezy's friction law, leads to the governing unsteady flow equation as:

$$I - Q = \frac{d}{dt}\left[K\left(Q + \theta\left(I - Q\right)\right)\right] \qquad \ldots(57)$$

in which,

$$K = \frac{\Delta x}{\left[\frac{5}{3} - \frac{4}{3}\frac{R_3}{\frac{\partial A}{\partial y}\big|_3}\sqrt{1+Z^2}\right] v_3} \qquad \ldots(74)$$

and

$$\theta = \tfrac{1}{2} - Q_n\left\{\tfrac{1}{2} + \frac{1}{8}G + \frac{1}{16}G^2 + \frac{5}{128}G^3 + \ldots.\right\} \frac{\left[1 - \frac{4}{9}F^2\left(1-2\frac{R_m}{\frac{\partial A}{\partial y}\big|_m}\sqrt{1+Z^2}\right)^2\right]}{v_m S_o \frac{\partial A}{\partial y}\big|_m\left[\frac{5}{3} - \frac{4}{3}\frac{Rm}{\frac{\partial A}{\partial y}\big|_m}\sqrt{1+Z^2}\right]\Delta x} \qquad \ldots(75)$$

Where,

R_3 = hydraulic radius at section (3)

$\frac{\partial A}{\partial y}|_{\bar{3}}$ top width of flow at section (3)

v_3 = velocity of flow at section (3)

v_m = velocity of flow at mid section of the routing reach

R_m = hydraulic radius at mid-section of the routing reach

$\frac{\partial A}{\partial y}|_m$ = top width of flow at midsection of the routing reach

Q_n = Q3 the flow at section (3)

Expressing K and θ in terms of flow variable and neglecting G_m, G_m^2, G_m^3 .....etc.

$$K = \frac{\Delta x}{v_3\left[\frac{5}{3}-\frac{4}{3}\frac{(B + y_3Z)\, y_3\, \sqrt{1+Z^2}}{(B+2y_3\sqrt{1+Z^2})(B+2y_3Z)}\right]} \qquad \ldots(76)$$

and

$$\theta = \tfrac{1}{2} - \frac{Q_3\left[1-\frac{4}{9}F^2\left(1-\frac{2(B + y_mZ)\, y_m\sqrt{1+Z^2}}{(B+2y_m\sqrt{1+Z^2})(B+2y_mZ)}\right)^2\right]}{2S_o v_m(B+2y_mZ)\left[\frac{5}{3} - \frac{4}{3}\frac{(B+y_mZ)y_m\sqrt{1+Z^2}}{(B+2y_m\sqrt{1+Z^2})(B+2y_mZ)}\right]\Delta x} \qquad \ldots(77)$$

K and θ expressed by Equations (76) and (77) have been used in this study.

Reducing K and θ for rectangular cross-section channel case:

For rectangular cross section Z = 0

when,

Z = 0, equations (76) and (77) reduce to:

$$K = \frac{\Delta x}{v_3\left[\frac{5}{3} - \frac{4}{3}\frac{y_3}{B + 2y_3}\right]} \qquad \ldots(78)$$

and

$$\theta = \tfrac{1}{2} - \frac{Q_3\left[\,1 - \frac{4}{9}F^2\left(\frac{B}{B + 2y_m}\right)^2\right]}{2B S_o\, v_m\left[\,\frac{5}{3} - \frac{4}{3}\,\frac{y_m}{B+2y_m}\right]\Delta x} \qquad \ldots(79)$$

Equations (78) and (79) were obtained in the earlier study (Perumal, 1986-87) of simplified hydraulic method for routing floods in uniform rectangular channels with constant bed slope.

5.0 APPLICATION

The methodology described above was verified by applying it for routing floods in trapezoidal channels assuming that the flow follows Manning's friction law. It was assumed that the routing parameters K and θ can be represented in terms of channel and flow parameters by equation (76) and (77) respectively.

It was considered that the approximation involved in computing θ using approximate 'ℓ' the distance between the mid-section and the section downstream of it where the normal discharge corresponding to the observed depth at mid-section is realized at the same instant of time, would not affect the accuracy of routing solution based on this procedure.

5.1 Test Series

The best approach for verifying the suggested methodology is to use hypothetical inflow-outflow hydrographs. Accordingly a hydrograph defined by a mathematical function is routed through the given channel for a specified distance using St.Venant's equations, which govern the one-dimensional flow in open channels, and thus the "observed" outflow hydrograph at the end of the specified distance is established. Now the same inflow hydrograph is routed in the same channel using the suggested procedure for the same specified distance and the resulting routed hydrograph is compared with the corresponding St. Venant's solution. The criteria for comparison based on various characteristics of outflow hydrograph are defined at section 5.3. The logic behind the use of hypothetical inflow-

outflow hydrographs for verifying such methodologies has been already established (Kundzewicz,1986).

5.1.1 Inflow hydrographs

In order to get a better understanding of the suggested procedure and for the purpose of effective comparison of various outputs obtained based on this procedure, it was decided to use the same inflow hydrograph in all the test runs. The hypothetical inflow hydrograph defined by a four parameter Pearson type-III distribution which is expressed by the following equation was adopted in this study:

$$Q(t) = Q_b + (Q_p - Q_b)\left(\frac{t}{t_p}\right)^{\frac{1}{(\gamma - 1)}} e^{\frac{1}{(\gamma-1)}(1-t/t_p)} \qquad \ldots(80)$$

where,

Q_b	=	base flow	= 100 m^3/S
Q_p	=	peak flow	= 1000 m^3/S
t_p	=	time to peak	= 10 hours
γ	=	skewness factor	= 1.15

This hydrograph was addopted by Weinmann (1977) based on the consideration of steepness of hydrograph and magnitude of initial flow. The hydrograph based on equation (80) is shown in all the discharge hydrograph plots presented in this report. The same hydrograph was also used in the earlier study(Perumal 1986-97) for verifying the simplified routing method developed for routing floods in rectangular channels.

5.1.2 Channel geometry and flow resistance properties.

The trapezoidal channel with the bottom width of 50 m

and the side slope of Z=1.5(Z horizontal: 1 vertical) was used for all the test runs, and the routing computations were carried out for a maximum reach length of 40 km. The methodology was tested on four different channel configurations which are characterised by the following bed slope and friction values as given in Table - 1.

TABLE 1

CHANNEL CONFIGURATIONS

Channel type	bed slope	n - Value
1	0.0002	0.04
2	0.0002	0.02
3	0.002	0.04
4	0.002	0.02

These configurations were earlier adopted by Weinmann(1977) possibly due to the reason that the first two configurations represent worst cases for which the approximate routing procedures is expected to perform poorly, and the last two configurations represent the best cases for which it is expected to perform well.

5.2 Solution Procedure

The initial parameter values for K_o and θ_o were evaluated using equations (76) and (77) respectively. Using these parameter values, the coefficients of the conventional Muskingum method were evaluated as:

$$C_1 = \frac{-K\theta_o + \Delta t/2}{K(1-\theta_o) + \Delta t/2}$$

$$C_2 = \frac{K\theta_o + \Delta t/2}{K(1-\theta_o) + \Delta t/2} \qquad \ldots(81)$$

$$C_3 = \frac{K(1-\theta_o) - \Delta t/2}{K(1-\theta_o) + \Delta t/2}$$

Then the discharge Q_2 at the outflow section corresponding to inflow I_2, where I_2 corresponds to inflow ordinate at $t = \Delta t$, was evaluated as:

$$Q_2 = C_1 I_2 + C_2 I_1 + C_3 Q_1 \qquad \ldots(82)$$

Knowing I_2 and Q_2, the discharge at section (3) as dipicted in figure (2) was evaluated as:

$$Q_3 = Q_2 + \theta_o (I_2 - Q_2) \qquad \ldots(83)$$

Corresponding to this discharge, the normal depth at the middle of the reach was evaluated using Newton-Raphson method based on the normal depth-discharge relationship as:

$$Q_3 = \frac{1}{n} \frac{[(B + y_m Z) y_m]^{5/3} S_o^{\frac{1}{2}}}{(B + 2y_m \sqrt{1+Z^2})^{2/3}} \qquad \ldots(84)$$

Then the discharge at the middle of the reach was evaluated as:

$$Q_m = (I_2 + Q_2)/2 \qquad \ldots(85)$$

Knowing Q_m, y_m, Q_3 and F^2, the new θ was computed using equation (77) corresponding to Q_2. Based on equation (66) the flow depth at section (3) was evaluated as:

$$y_3 = y_m + \frac{(Q_3 - Q_m)}{\left[\frac{5}{3}(B+2y_m Z) - \frac{4}{3} \frac{(B+y_m Z) y_m \sqrt{1+Z^2}}{(B+2y_m \sqrt{1+Z^2})}\right] \frac{Q_m}{y_m (B+y_m Z)}} \qquad \ldots(86)$$

The velocity v_3 at section (3) was computed as:

$$v_3 = \frac{Q_3}{y_3(B+y_3Z)} \qquad \ldots(87)$$

Knowing v_3 and y_3, and the distance of routing reach Δx, the new travel time K was computed using equation (76).

These revised K and θ values were used for the next step of solution corresponding to the new input ordinate. These steps were repeated for the entire solution procedure, thus varying the values of K and θ at every time step, but at the same time adopting the linear solution procedure. The flow depth at the outflow section corresponding to the solution Q_2 was computed as:

$$y_2 = y_m + \frac{(Q_2 - Q_m)}{\left[\frac{5}{3}(B+2y_mZ) - \frac{4}{3}\frac{y_m(B+y_mZ)\sqrt{1+Z^2}}{(B+2y_m\sqrt{1+Z^2})}\right]\frac{Q_m}{y_m(B+y_mZ)}} \qquad \ldots(88)$$

The procedure described above correspond to the variable parameters case. Two different approaches of solution procedures were adopted for the variable parameters case viz,

1) Considering the entire 40 km. reach as a single reach and

2) Considering it consists of number of sub-reaches. The other solution procedure corresponds to the case of adopting constant θ and variable K, along with the consideration of 40 km reach as a single reach.

In order to test whether linear interpolation of given inflow and routed outflow hydrographs at some downstream point is appropriate for finding the routed hydrograph at some intermediate points, two different cases were studied.

In order to check whether the interpolation solution yield comparable result with the direct routing solution for a distance of 5 km, the following procedure was adopted:

For the case of channel type-1, and channel type-2, the linear interpolation solution was obtained at the end of the reach length of 5 km. based on the given inflow hydrograph and the routed hydrograph at the end of 40 km. For comparison with this solution, the inflow hydrograph was routed for 5 km. by considering it as a single reach.

Sixteen test runs as indicated in Table-2 were made in order to have a better understanding of the proposed methodology. Runs based on different combination of parameter variations, and number of sub-reaches considerations were made. Such combinations tested are listed in the 'Remarks' column of Table-2. In all the runs, the routing time intervals Δt was considered as 15 minutes in order to avoid any numerical error in the solution using equation (82).

TABLE 2

TEST RUN DETAILS

Test Run No.	Channel Type	Required Reach Length in (Km.)	Adopted Reach Length in (Km)	No. of Sub-reaches	Length of sub-reach	Remarks
1	1	40	40	1	40	*
2	1	40	40	1	40	**
3	1	40	40	8	5	*
4	2	40	40	1	40	*
5	2	40	40	1	40	**
6	2	40	40	8	5	*
7	3	40	40	1	40	*
8	3	40	40	1	40	**
9	3	40	40	8	5	*
10	4	40	40	1	40	*
11	4	40	40	1	40	**
12	4	40	40	8	5	*
13	1	5	40	1	40	***& *
14	1	5	5	1	5	*
15	2	5	40	1	40	***& *
16	2	5	5	1	5	*

Note: * Both θ and K varying
** Only K varying and θ remaining constant
*** Solution was obtained by linear interpolation of inflow and routed outflow hydrographs.

5.3 Comparison Criteria

The following comparison criteria were adopted for checking the efficiency of the proposed method of solution in comparison with the St. Venant's solution:

5.3.1 The hydrograph fitting consideration

The closeness with which the proposed method of solution follows the true solution, including the closeness of shape and size of hydrograph, can be measured using the criteria of variance explained by the method. The expression for variance explained in % is given as:

$$\text{Variance explained in (\%)} = \frac{\text{(Total Variance-Remaining Variance)}}{\text{Total variance}} \times 100 \quad \ldots(89)$$

where,

$$\text{the total variance} = \frac{1}{N}\sum_{i=1}^{N} (Q_{oi} - \bar{Q}_{oi})^2 \quad \ldots(90)$$

$$\text{the remaining variance} = \frac{1}{N}\sum_{i=1}^{N} (Q_{oi} - Q_{ci})^2 \quad \ldots(91)$$

with,

Q_{oi} = the i^{th} discharge observation

$\bar{Q}_{oi}$ = mean of the discharge observation.

Q_{ci} = the i^{th} discharge computed using the proposed method

N = the total number of discharge ordinates.

5.3.2 Magnitude of flood peak consideration

Relative error in peak discharge (%) is given as:

$$Q_{PE} = \frac{(Q_{pc} \quad Q_{po})}{Q_{po}} \times 100 \qquad \ldots(92)$$

where,

Q_{pc} = the computed peak outflow discharge

Q_{po} = the observed peak outflow discharge

Error in peak stage (metre) is given as:

$$Y_{PE} \pm y_{pc} - y_{po} \qquad \ldots(93)$$

where,

y_{pc} = computed peak stage at the outflow section

y_{po} = observed peak stage at the outflow section.

5.3.3 Time of peak consideration

Error in time of peak discharge(hours) is given as:

$$T_{PQE} = t\,(Q_{pc}) - t(Q_{po}) \qquad \ldots(94)$$

where,

$t(Q_{pc})$= time corresponding to computed peak discharge

$t(Q_{po})$= time corresponding to observed peak discharge.

Error in time of peak stage (meters) is given as:

$$T_{PYE} = t(y_{pc}) - t(y_{po}) \qquad \ldots(95)$$

where,

$t(y_{pc})$= time corresponding to computed peak stage at the out flow section.

$t(y_{po})$= time corresponding to observed peak stage at the outflow section.

5.3.4 Conservation of mass consideration

The relative error in the flow volume in percent of the

total inflow volume is expressed as:

$$EVOL = \left[\frac{\sum_{i=1}^{N} Q_{ci} - \sum_{i=1}^{N} I_i}{\sum_{i=1}^{N} I_i} \right] \times 100 \qquad \ldots(96)$$

where,

I_i = the i^{th} inflow discharge.

6.0 RESULTS AND DISCUSSIONS

6.1 Results

Table-3 presents the results of variance explained, relative errors in peak discharge and peak stage, errors in time to peak discharges and peak stages, and the relative error in flow volume for all 16 test runs made in this study. Figure(3) shows the inflow hydrographs, and the outflow hydrographs, computed from test run nos 1, 2 amd 3 and from St. Venant's equations (the " Observed " hydrographs) Figure (4) shows the corresponding computed stage hydrographs at the outflow section. Similarly figures (5),(7) and (9) respectively show the inflow hydrographs,and the outflow hydrographs computed from test run number 4-6, 7-9 and 10-12 along with the St. Venant's solutions for these runs. Fugures (6), (8) and (10) respectively show the computed stage hydrographs at the outflow sections along with the concerned stage hydrographs due to St. Venant's solutions for the above mentioned runs. Figures (11),(12), (13) and (14) respectively show the variation of the travel time parameter K vs. the corresponding given inflow ordinates for test run nos. 1,4,7 and 10. Figures (15), (16) (17) and (18) respectively show the variation of the weighting factor θ vs the corresponding given inflow ordinates for test run nos. 1,4,7 and 10. Figure (19) shows the inflow hydrographs, the computed outflow hydrographs, and the corresponding St. Venant's solution from test run No 13 and 14 corresponding to channel type-I. The computed discharge hydrograph at section (3) corresponding to test run No. 14 has also been plotted

TABLE - 3

COMPARISON OF RESULTS

Test Run No.	Channel Type	Variance * explained in (%)	Q_{PE}^{**}	Y_{PE}^{**} (mt.)	T_{PQE}^{+} (hr)	T_{PYE}^{+} (hr)	$EVOL^{++}$
1	1	96.48	-2.37	1.06	-0.25	0.50	1.52
2	1	94.55	8.17	1.46	0.00	-0.25	8.24
3	1	98.09	-9.10	-0.11	0.25	1.25	2.09
4	2	99.04	-0.90	0.32	0.00	0.00	0.24
5	2	98.80	3.84	0.44	0.00	-0.25	2.93
6	2	99.82	-2.26	0.05	0.25	0.50	0.25
7	3	99.10	-1.41	-0.02	0.00	0.00	-0.30
8	3	99.11	-1.11	-0.02	0.00	0.00	-0.15
9	3	99.98	0.00	0.00	0.00	0.00	-0.42
10	4	99.89	-0.40	-0.01	0.00	0.00	-0.00
11	4	99.90	-0.40	0.00	0.00	0.00	-0.20
12	4	99.99	0.00	0.00	-0.00	0.00	-0.28
13	1	98.81	-5.01	-0.47	-0.25	0.25	0.19
14	1	99.73	-3.17	-0.48	-0.25	1.50	0.49
15	2	99.74	-0.03	-0.18	-0.25	0.25	0.03
16	2	99.98	-1.11	-0.08	0.00	0.75	0.05

* Reference : section 5.3.1.

** Reference : section 5.3.2

\+ Reference : section 5.3.3.

++ Reference : section 5.3.4.

to demonstrate that this hydrograph is observed downstream of section (2), i.e, the outflow section, indicating the negative value of the parameter θ. The outflow hydrograph computed from test run No. 13 for the reach length of 5 km, was obtained by interpolation of the given inflow hydrograph and the corresponding computed outflow hydrograph at 40 km. using the developed procedure. The outflow hydrograph computed from test run No.14 was obtained by directly routing the inflow hydrograph using the developed procedure for the same reach length of 5 km. Figure 20 shows the computed and St. Venant's solution stage hydrographs corresponding to test run No. 13 and 14. The computed stage hydrograph of test run No. 13 was obtained by linear interpolation of the "observed" stage hydrograph at the inflow section and the computed stage hydrograph at 40 km. using the developed procedure. The computed stage hydrograph of test run No. 14 was obtained by directly routing the inflow hydrograph for 5 km. using this procedure. Figure (21) shows the discharge hydrographs obtained from test run Nos. 15 and 16 corresponding to channel type II and they are similar to the results of test run Nos. 13 and 14. Figure (22) shows the stage hydrographs obtained from test run Nos. 15 and 16 corresponding to channel type-II and they are similar to the results of test run nos. 13 and 14. Figure (23) shows the variation of θ, corresponding to routing in the first reach length of 5 km of test run Nos. 3, with the inflow hydrograph ordinates. It can be seen that all the θ values are negative indicating the admissibility of negative values.

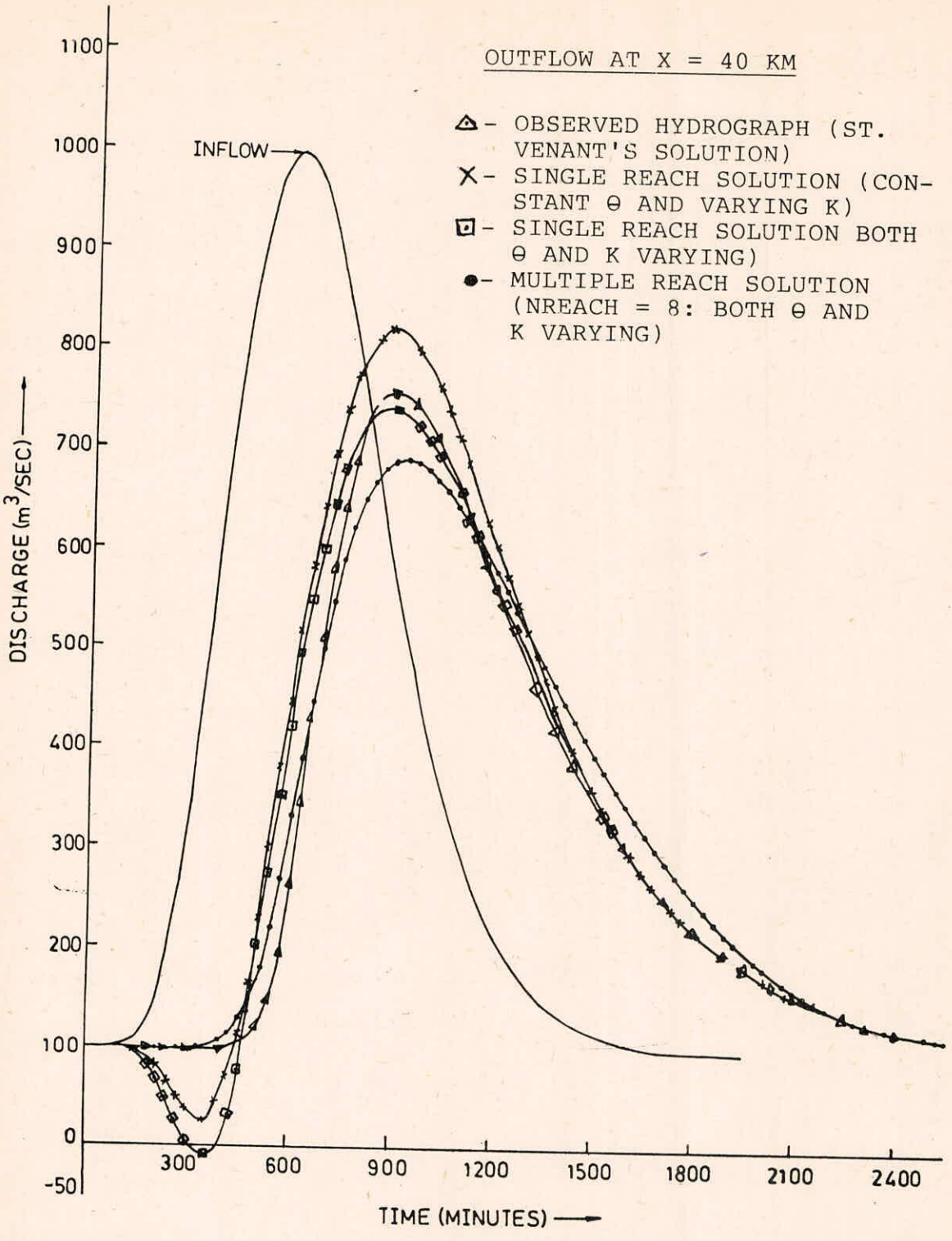

FIG.3 : OBSERVED AND COMPUTED DISCHARGE HYDROGRAPHS FOR CHANNEL TYPE-1.

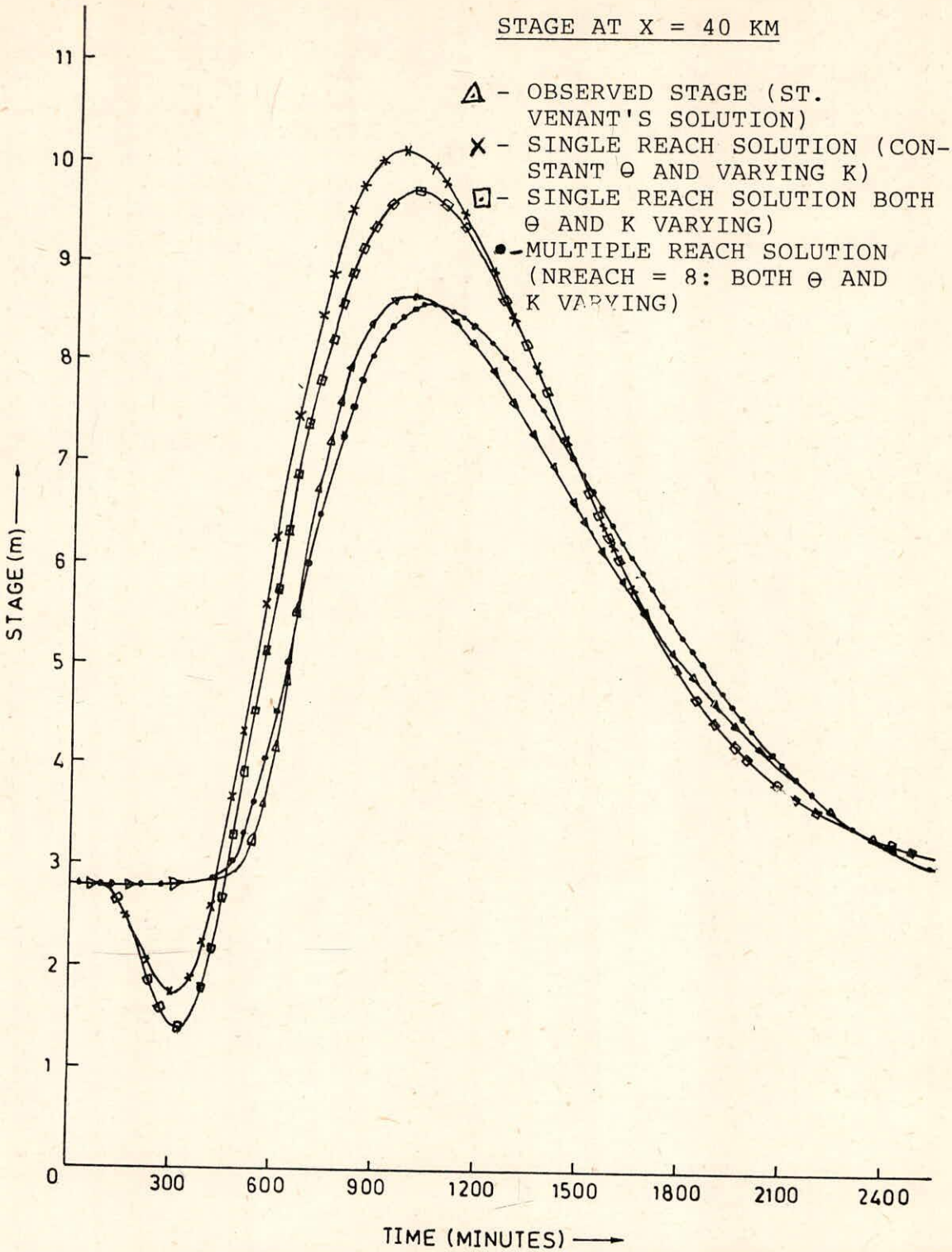

FIG.4 OBSERVED AND COMPUTED STATE HYDROGRAPHS FOR CHANNEL TYPE-1

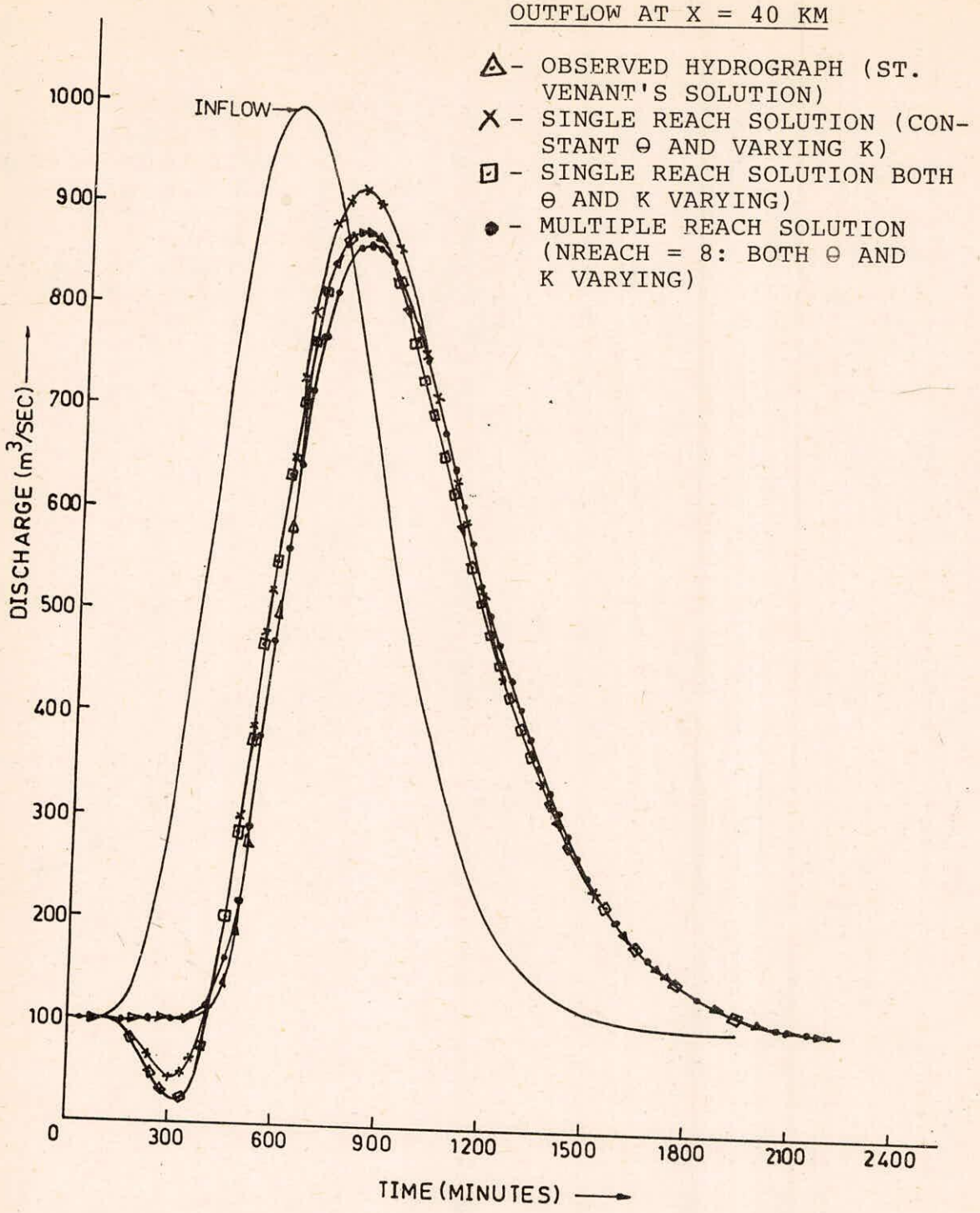

FIG.5 OBSERVED AND COMPUTED DISCHARGE HYDROGRAPHS FOR CHANNEL TYPE-2.

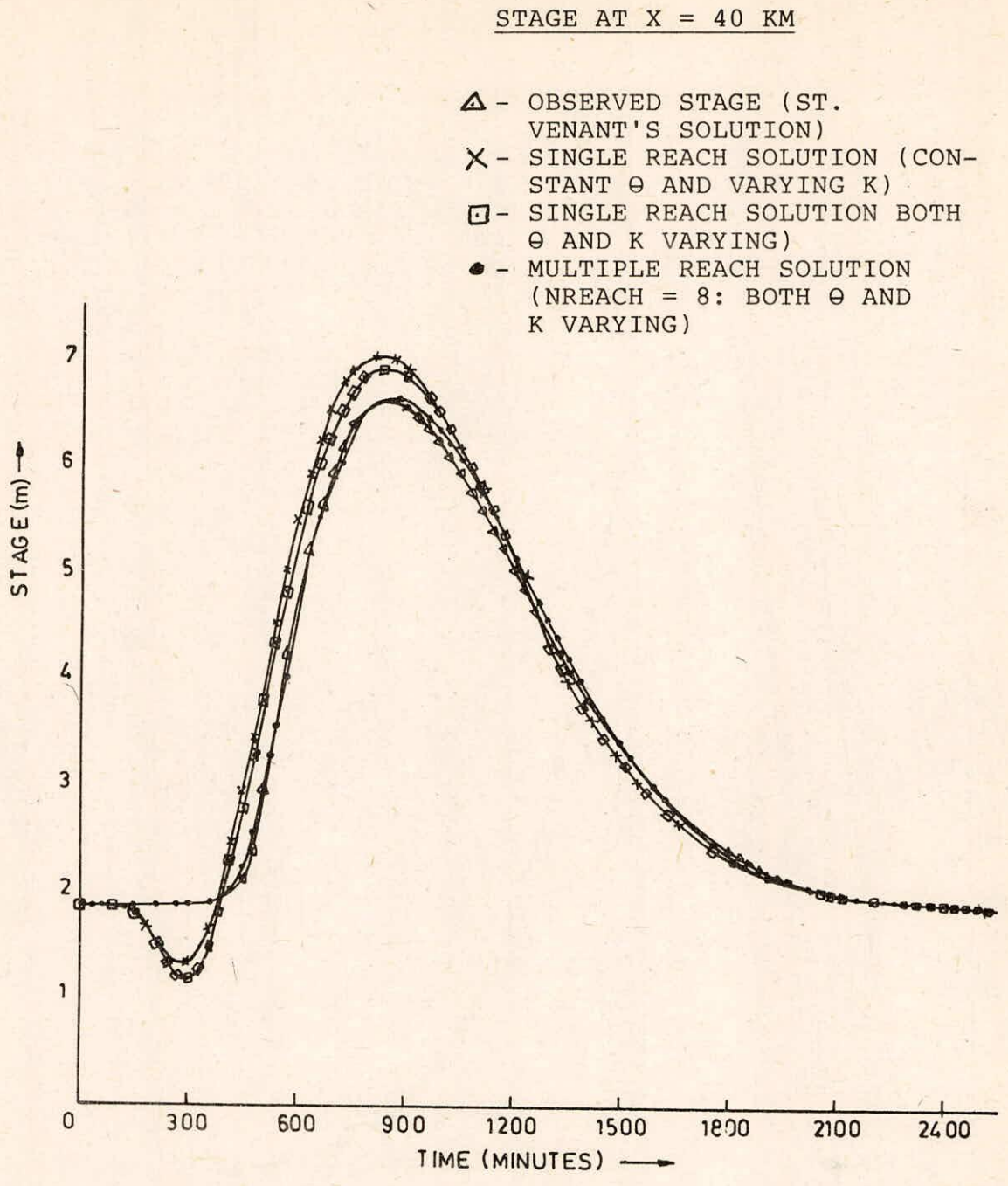

FIG.6 OBSERVED AND COMPUTED STAGE HYDROGRAPHS FOR CHANNEL TYPE - 2.

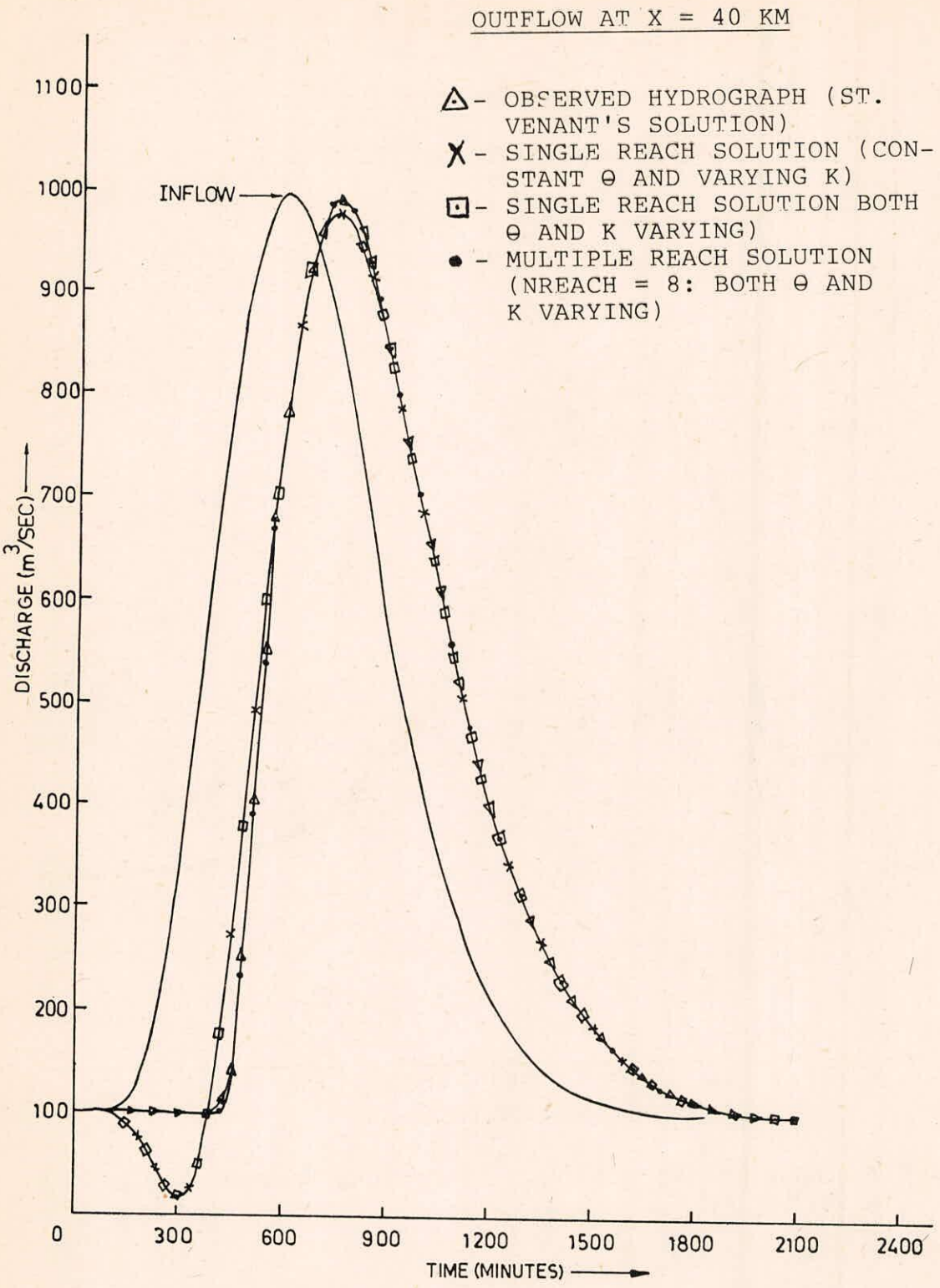

FIG.7 OBSERVED AND COMPUTED DISCHARGE HYDROGRAPHS FOR CHANNEL TYPE-3.

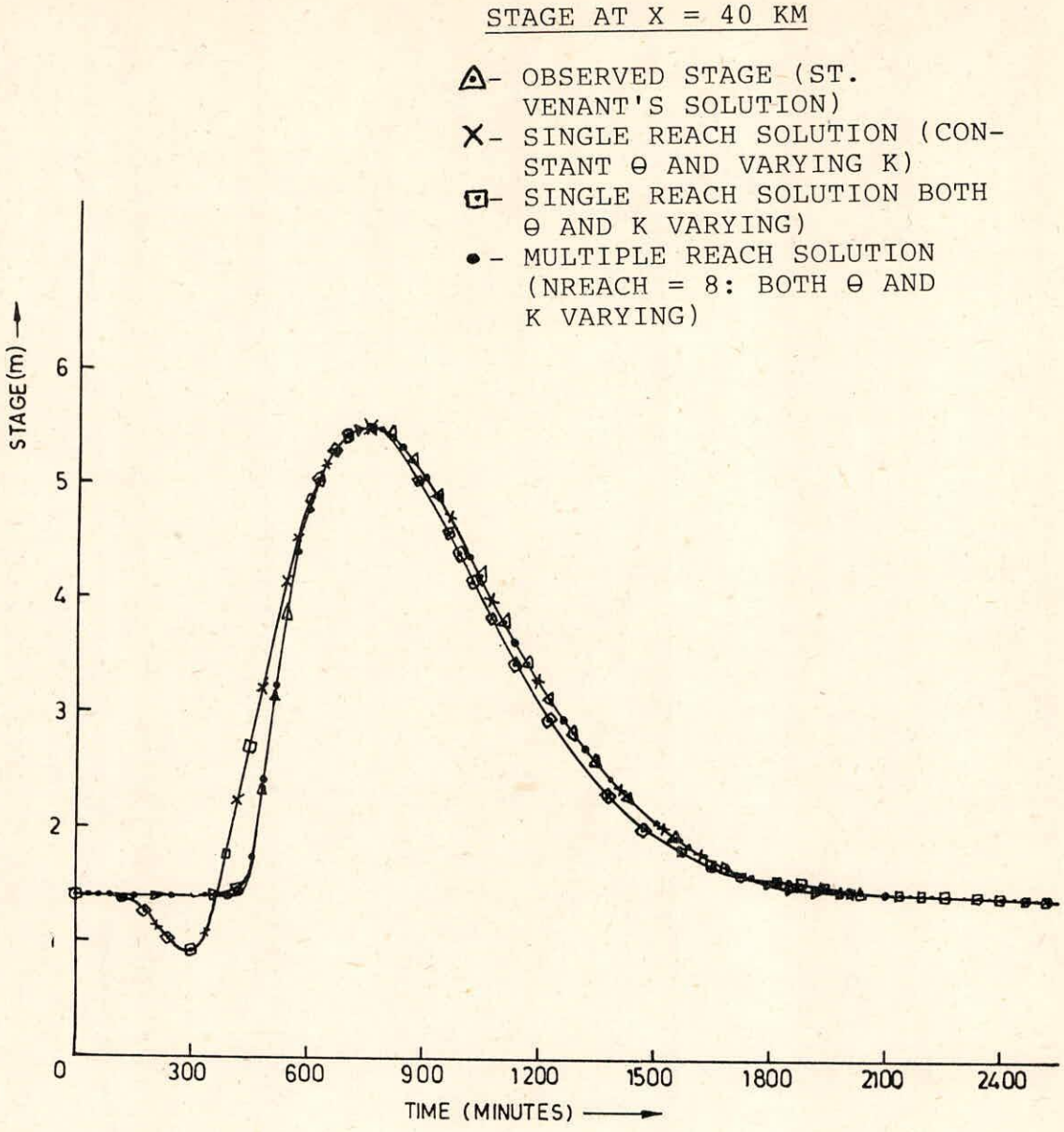

FIG.8 OBSERVED AND COMPUTED STAGE HYDROGRAPHS FOR CHANNEL TYPE-3.

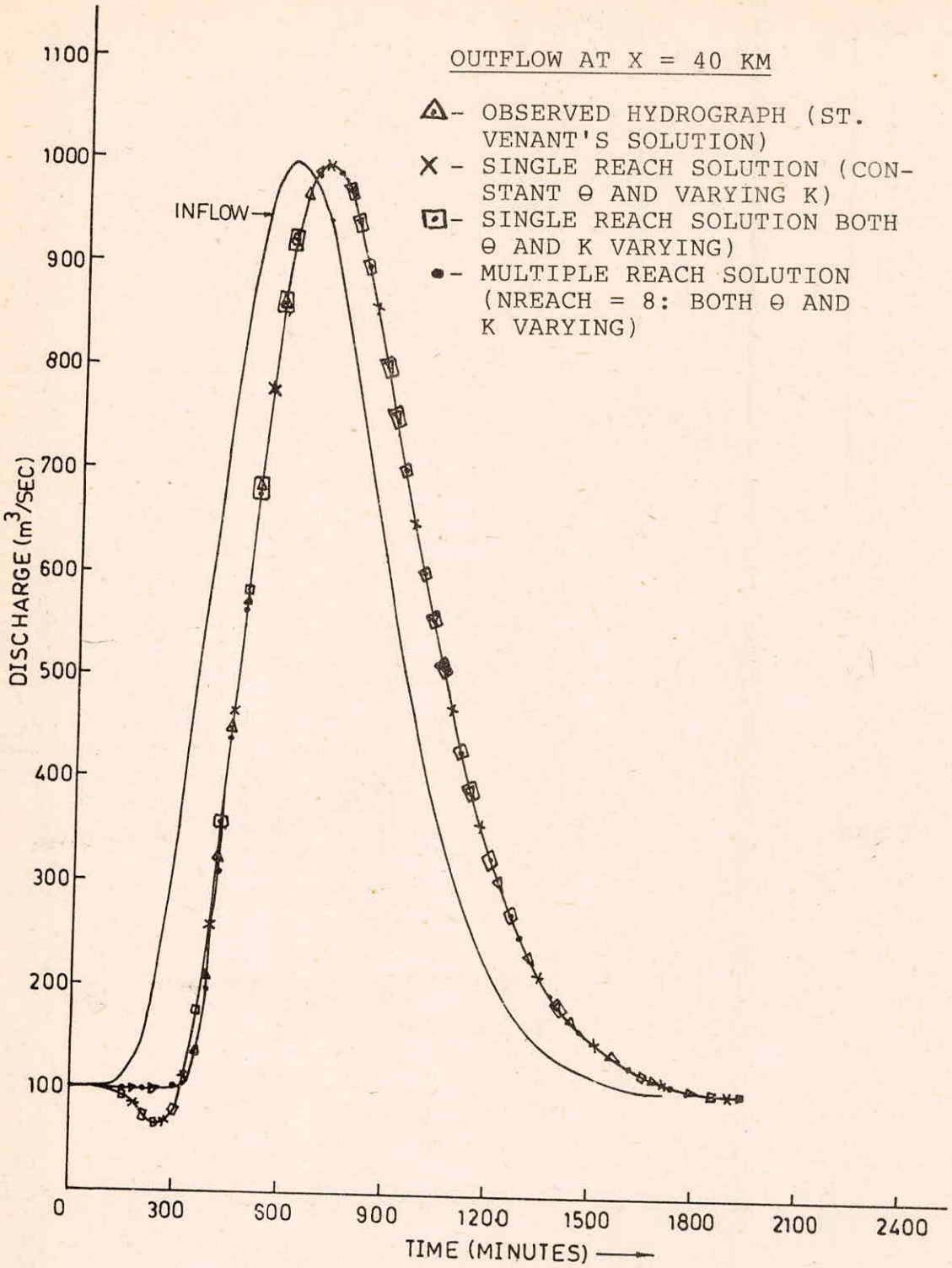

FIG.9 OBSERVED AND COMPUTED DISCHARGE HYDROGRAPHS FOR CHANNEL TYPE - 4.

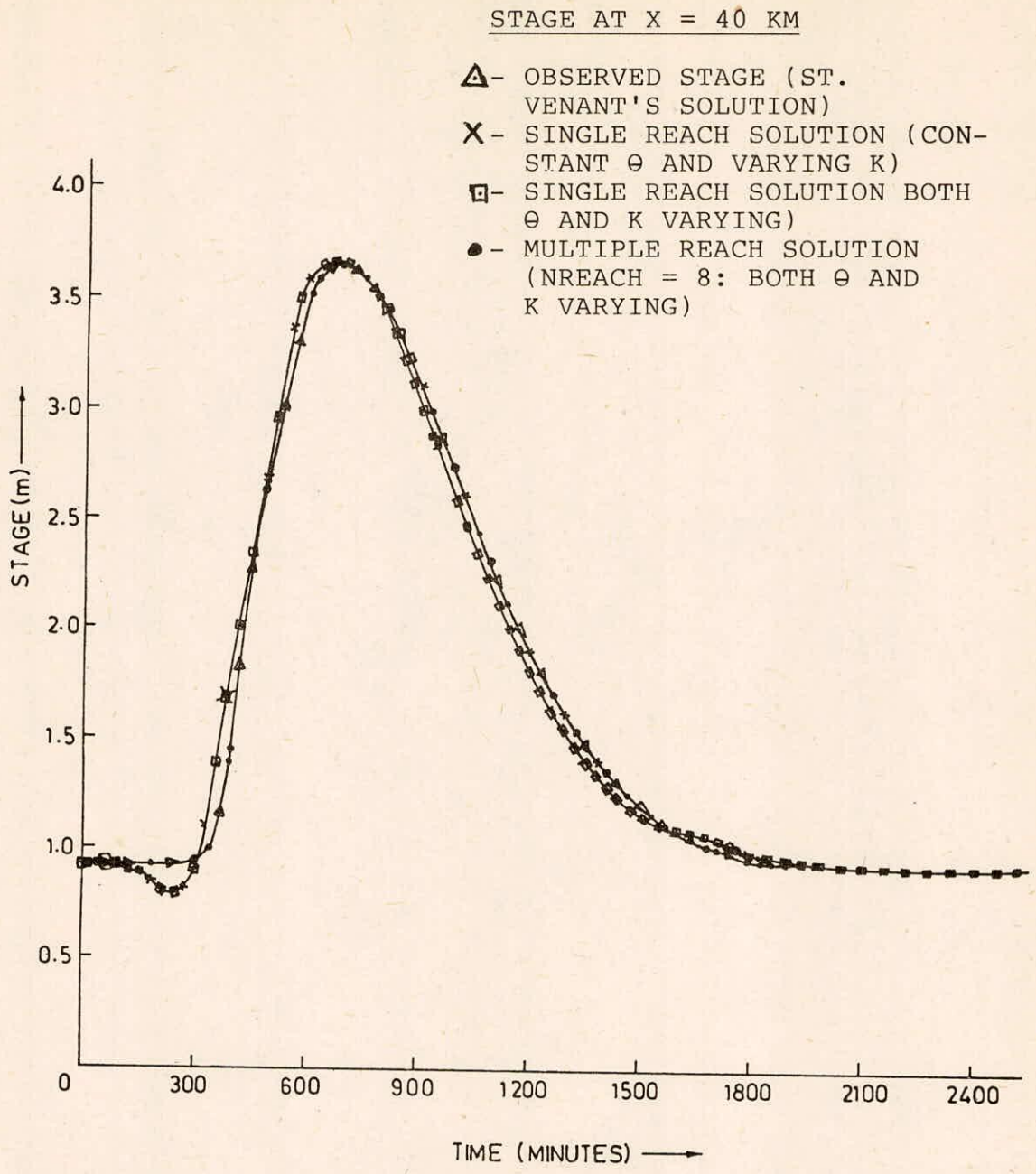

FIG.10 OBSERVED AND COMPUTED STAGE HYDROGRAPHS FOR CHANNEL TYPE-4.

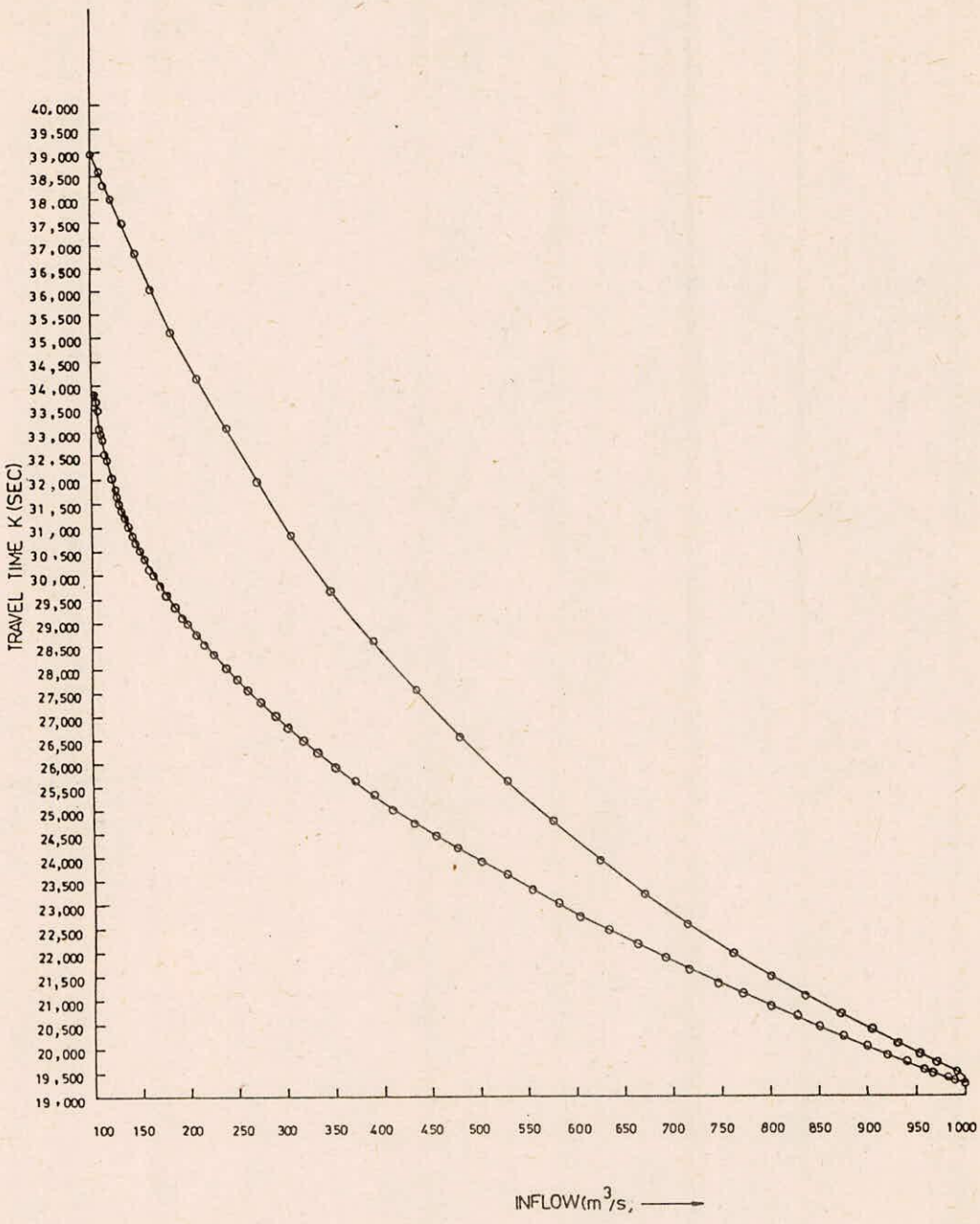

FIG.11 VARIATION OF TRAVEL TIME WITH INFLOW FOR CHANNEL TYPE-1.

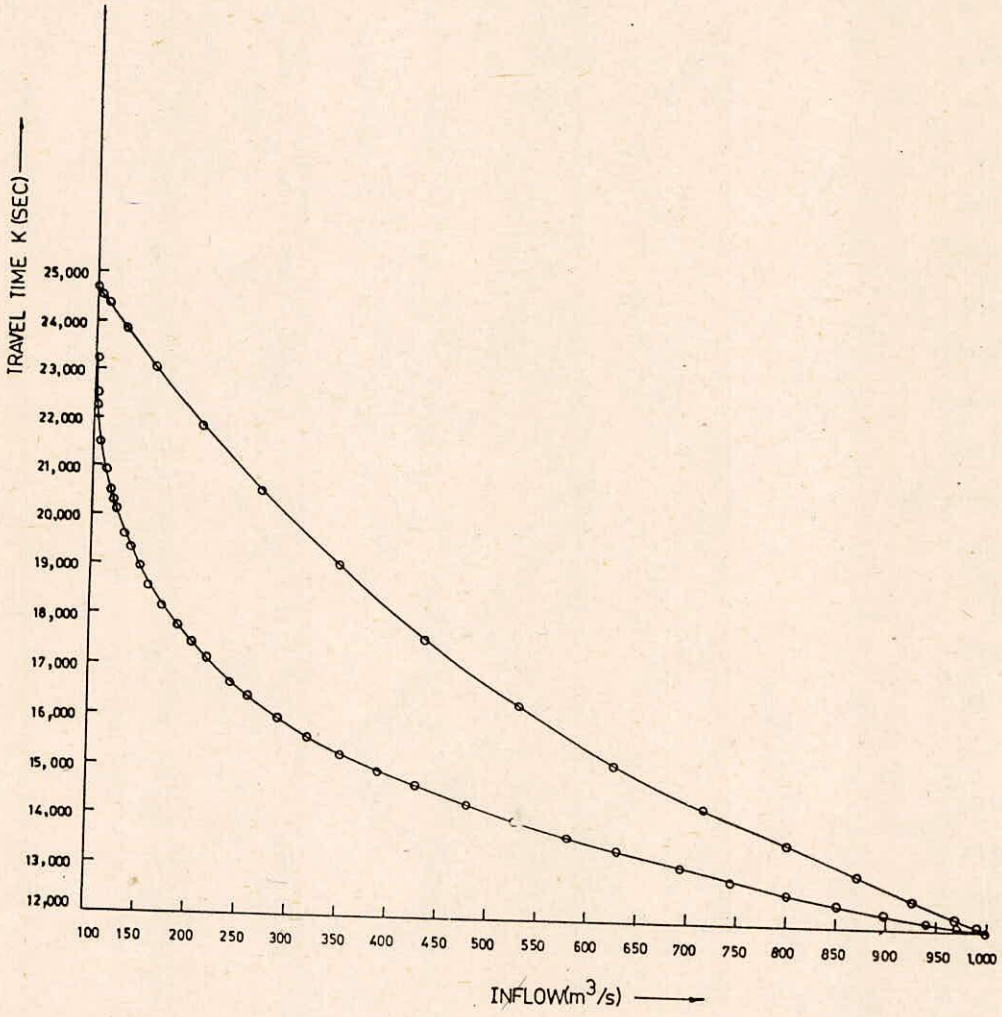

FIG.12 VARIATION OF TRAVEL TIME WITH INFLOW FOR CHANNEL TYPE-2.

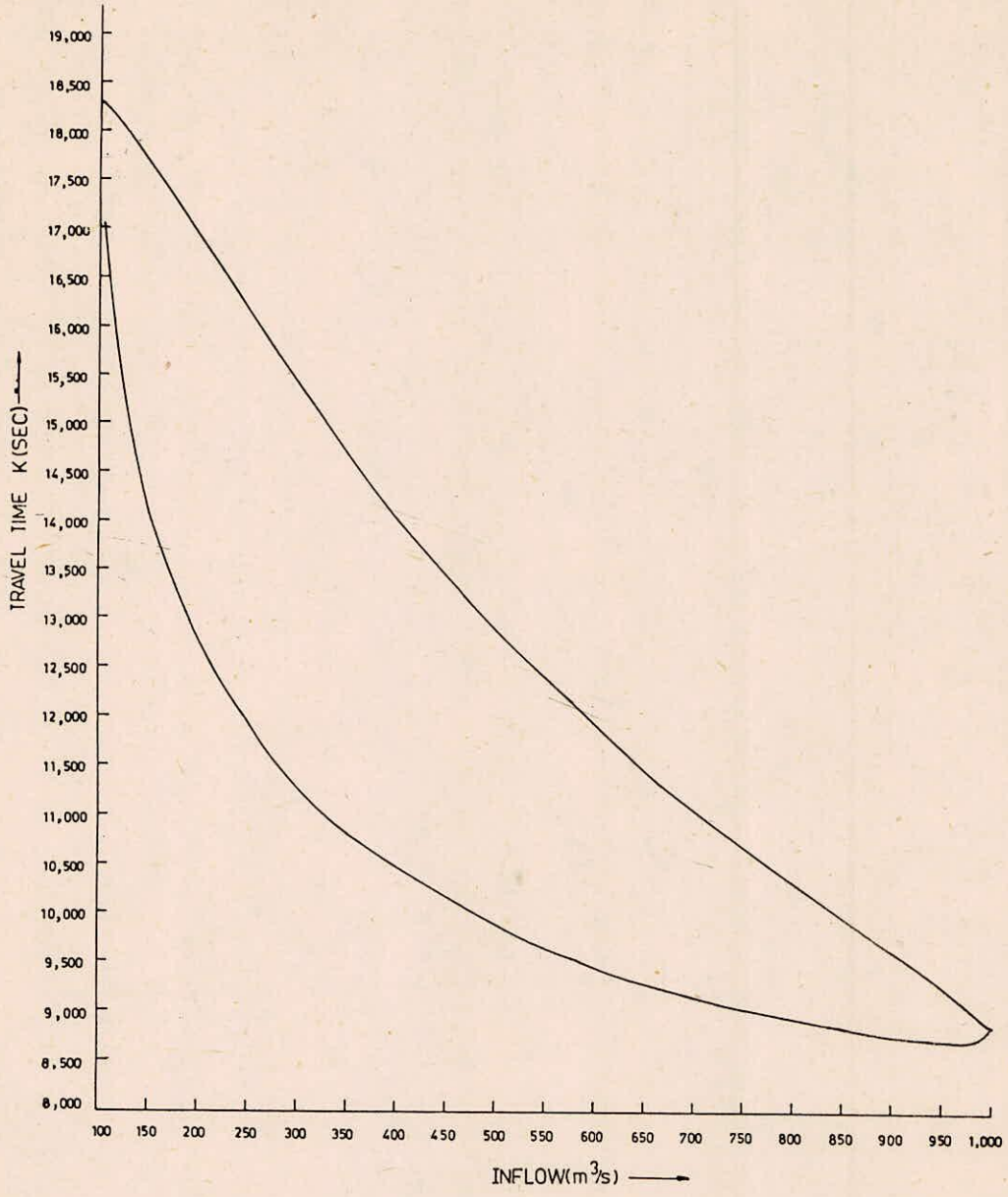

FIG.13 VARIATION OF TRAVEL TIME WITH INFLOW FOR CHANNEL TYPE-3.

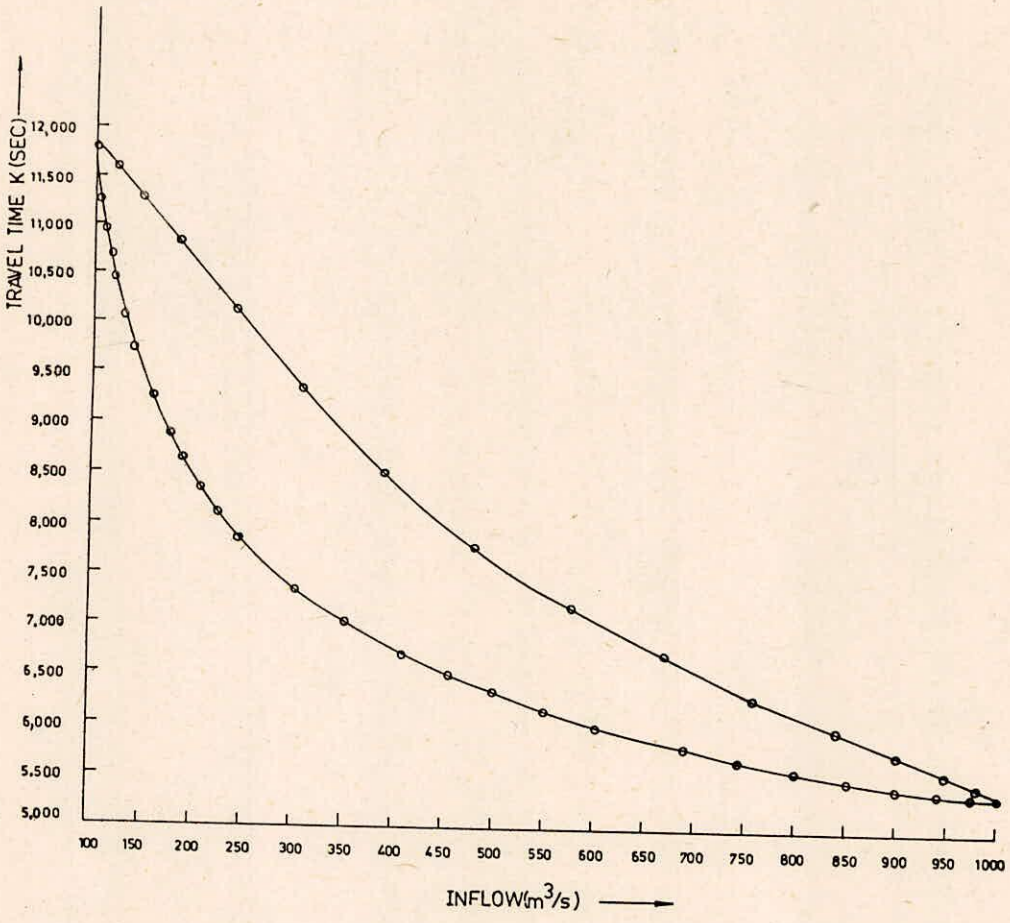

FIG.14 VARIATION OF TRAVEL TIME WITH INFLOW FOR CHANNEL TYPE-4.

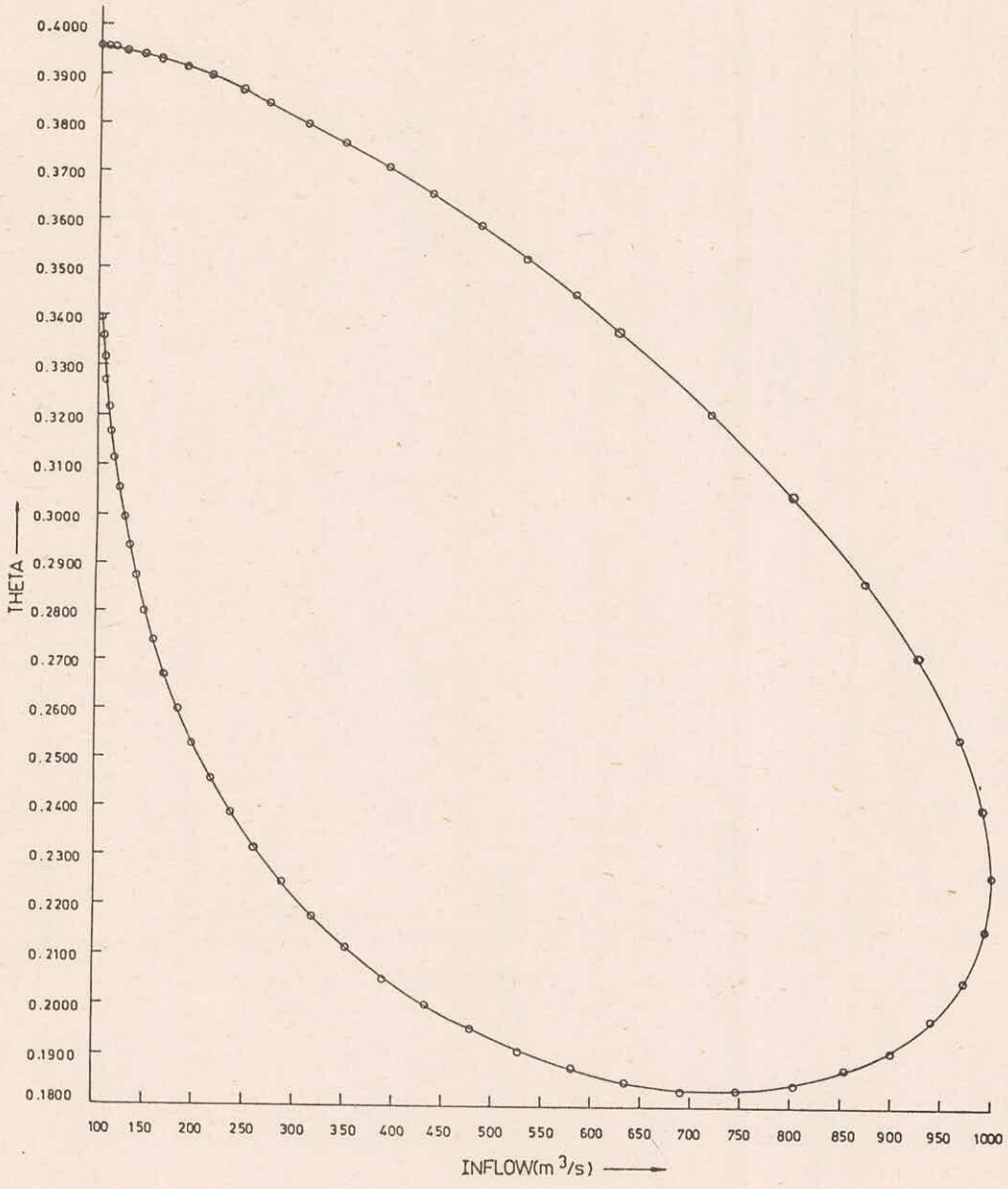

FIG.15 VARIATION OF Θ WITH INFLOW FOR CHANNEL TYPE-1

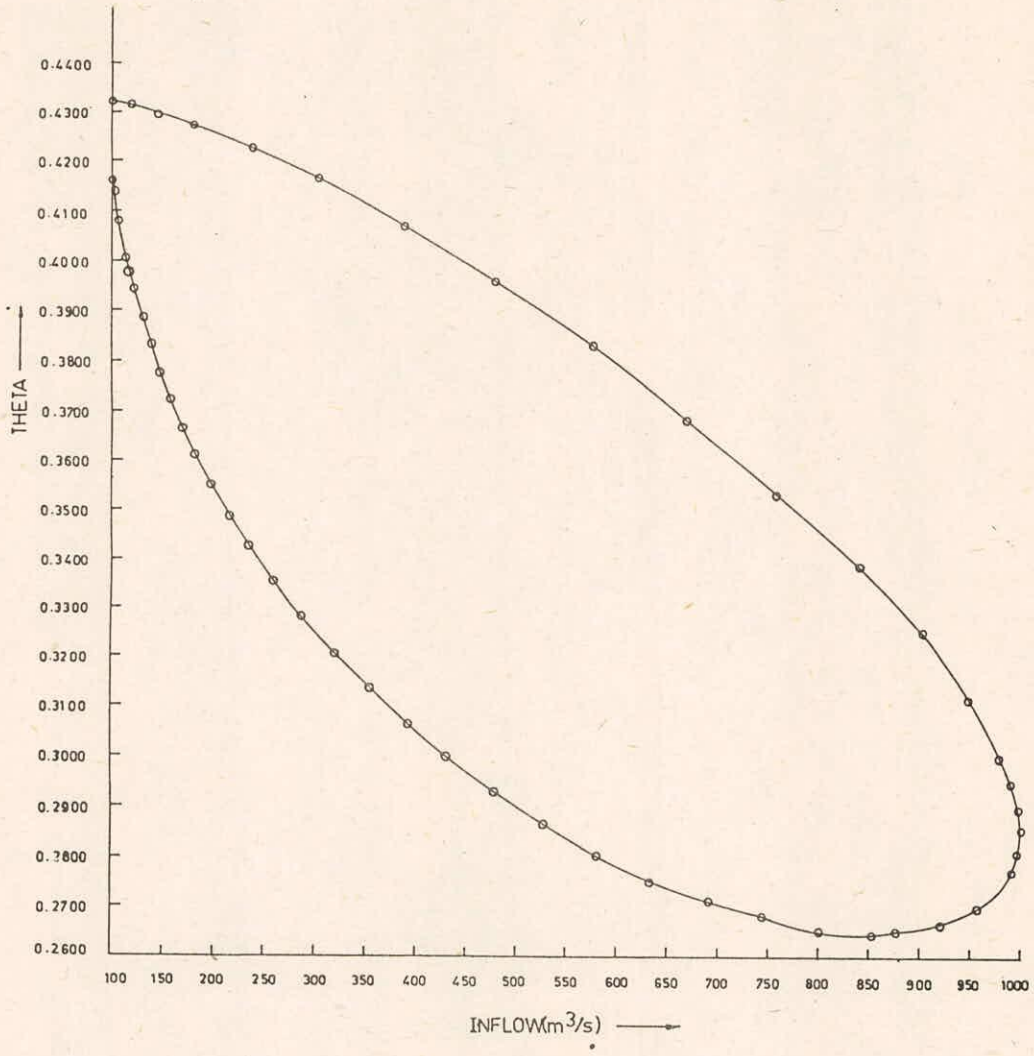

FIG.16 VARIATION OF θ WITH INFLOW FOR CHANNEL TYPE-2.

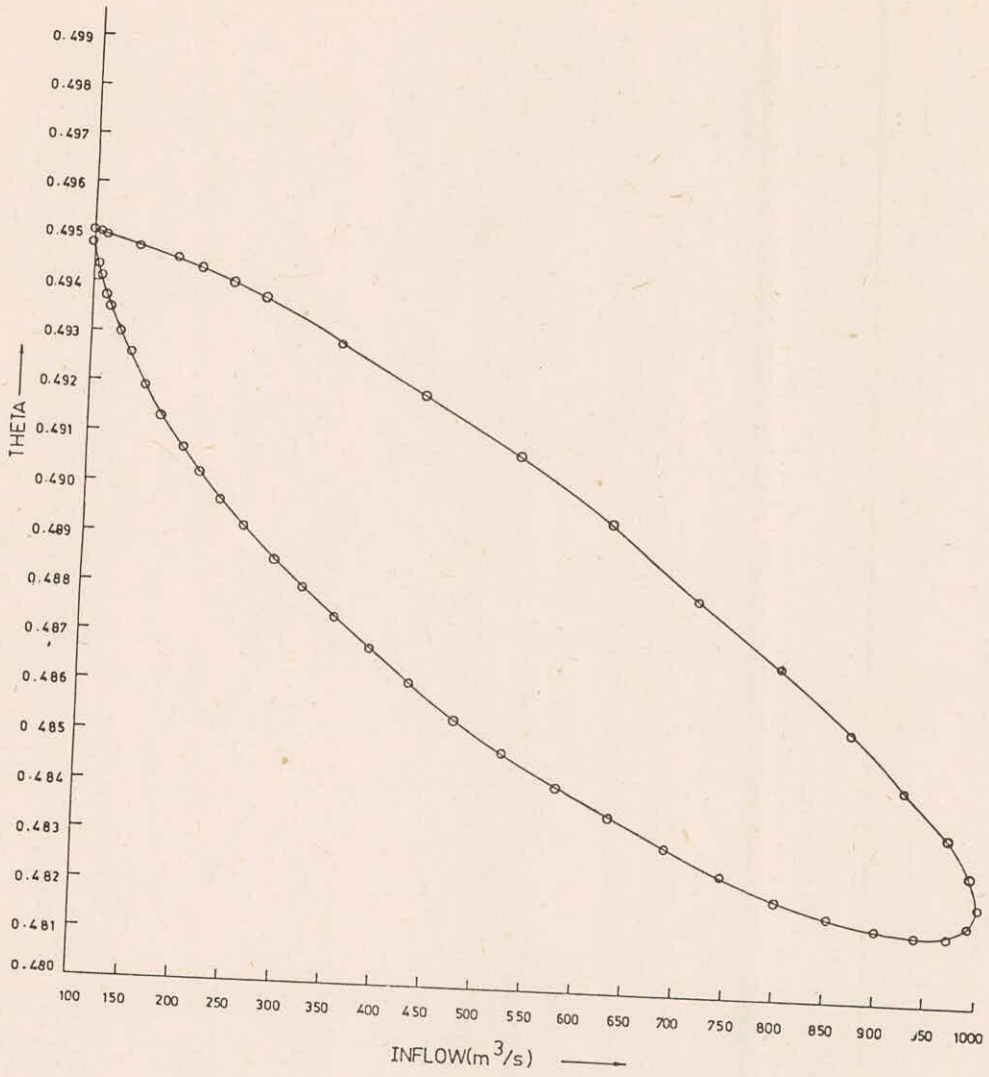

FIG.17 VARIATION OF θ WITH INFLOW FOR CHANNEL TYPE-3

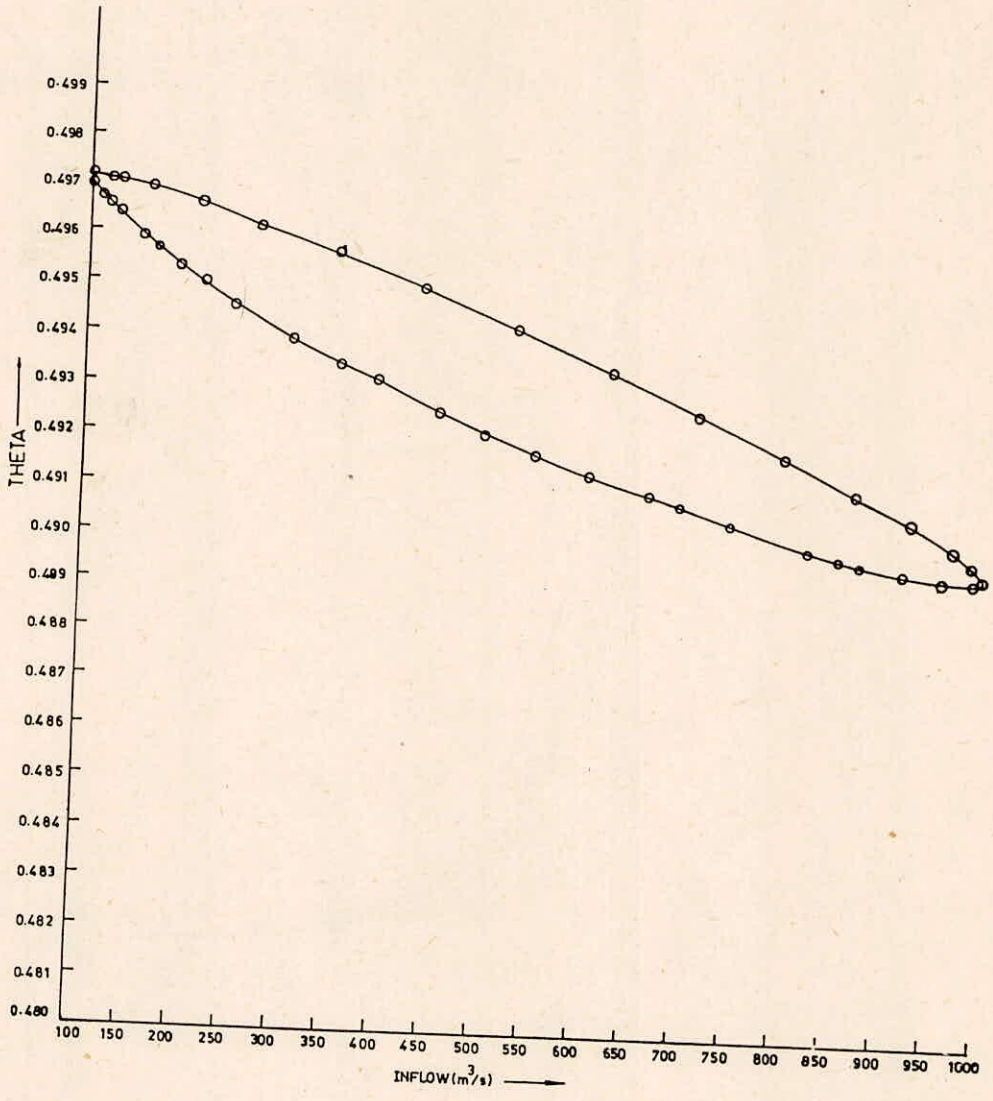

FIG.18 VARIATION OF Θ WITH INFLOW FOR CHANNEL TYPE-4

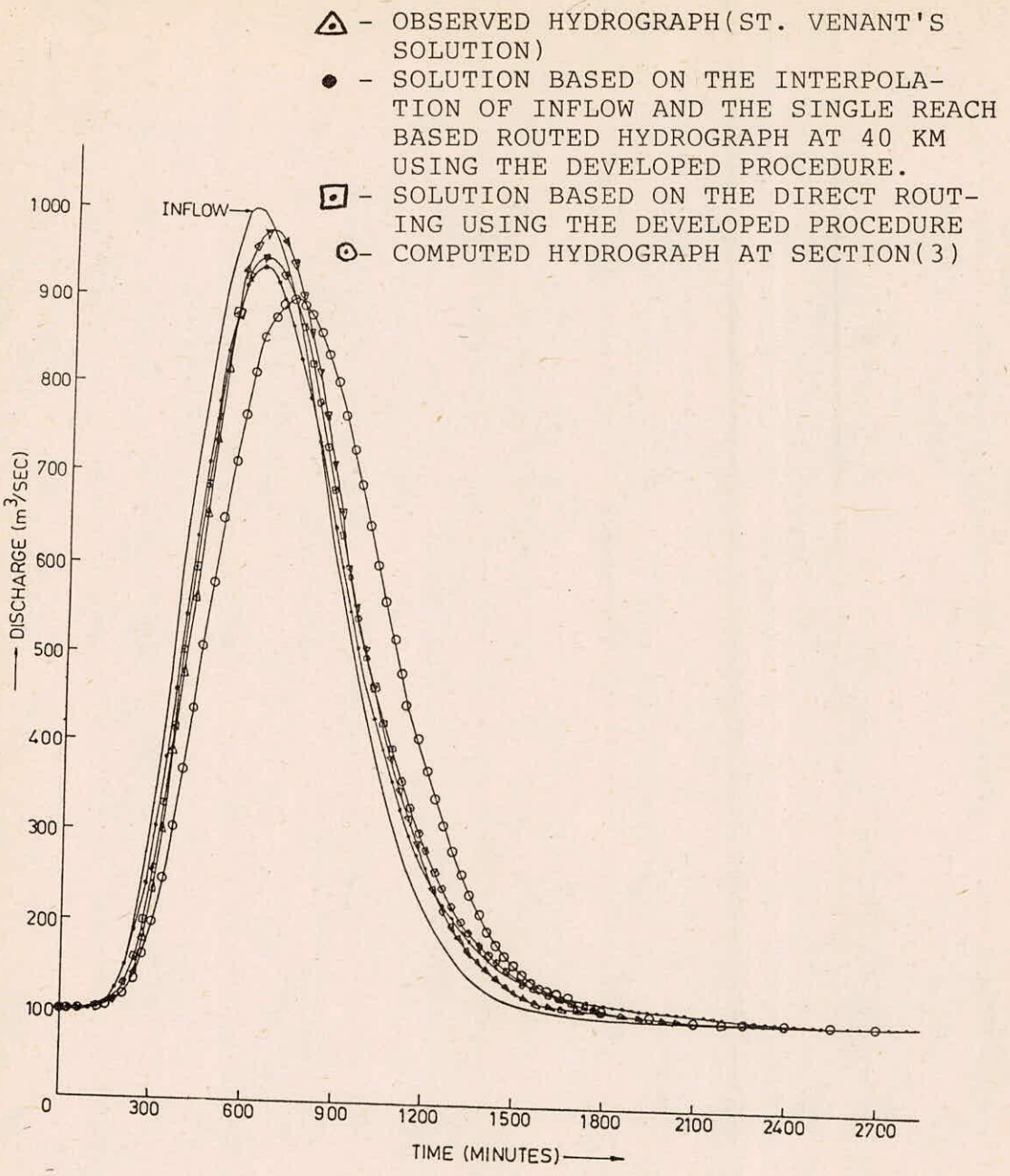

FIG.19 COMPARISON OF INTERPOLATED HYDROGRAPH AND DIRECTLY ROUTED HYDROGRAPH FOR 5 KM REACH (CHANNEL TYPE-1)

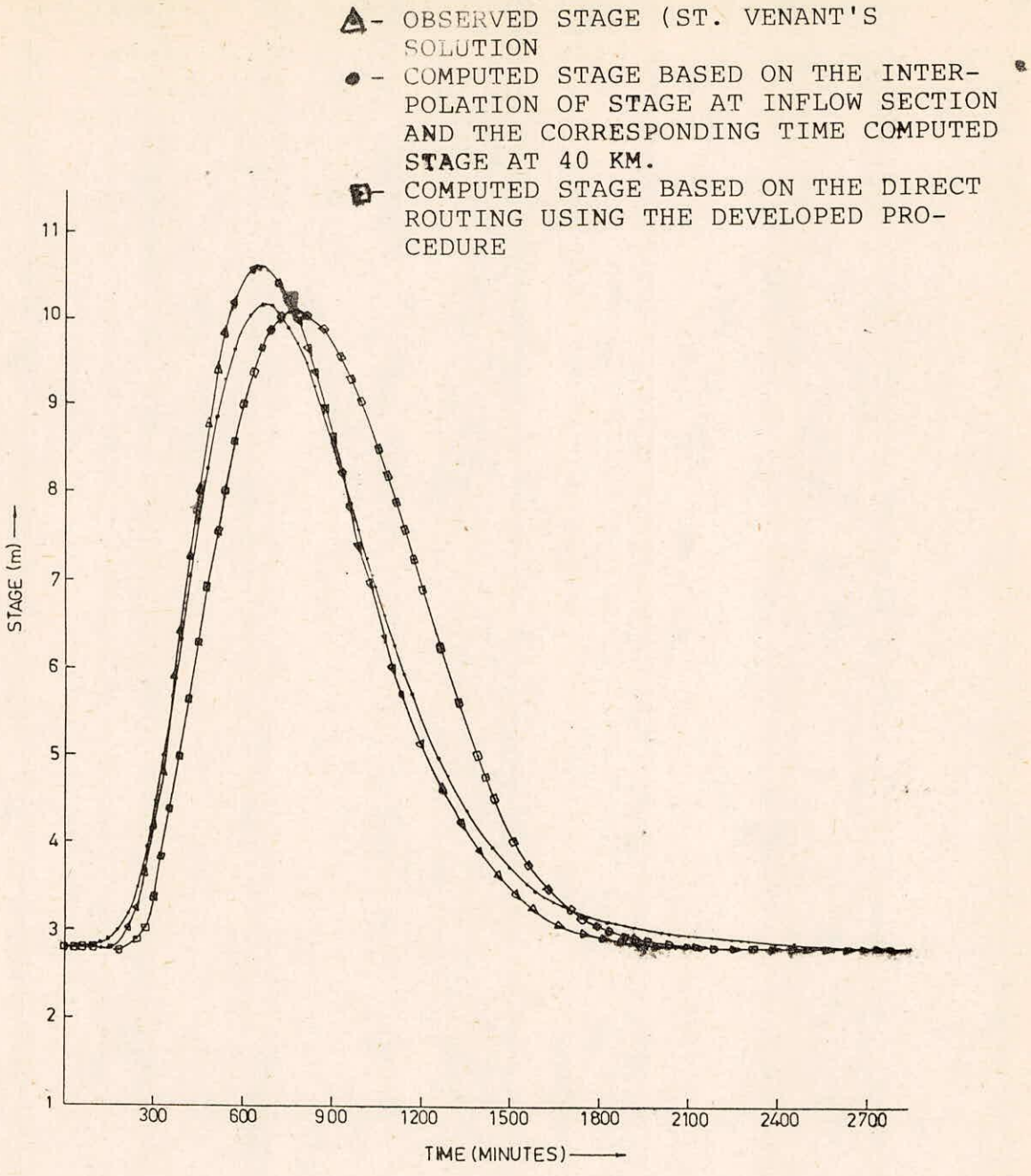

FIG.20 COMPARISON OF INTERPOLATED STAGE HYDROGRAPH AND THE STAGE HYDROGRAPH OBTAINED BY DIRECT ROUTING FOR 5 KM REACH (CHANNEL TYPE-1)

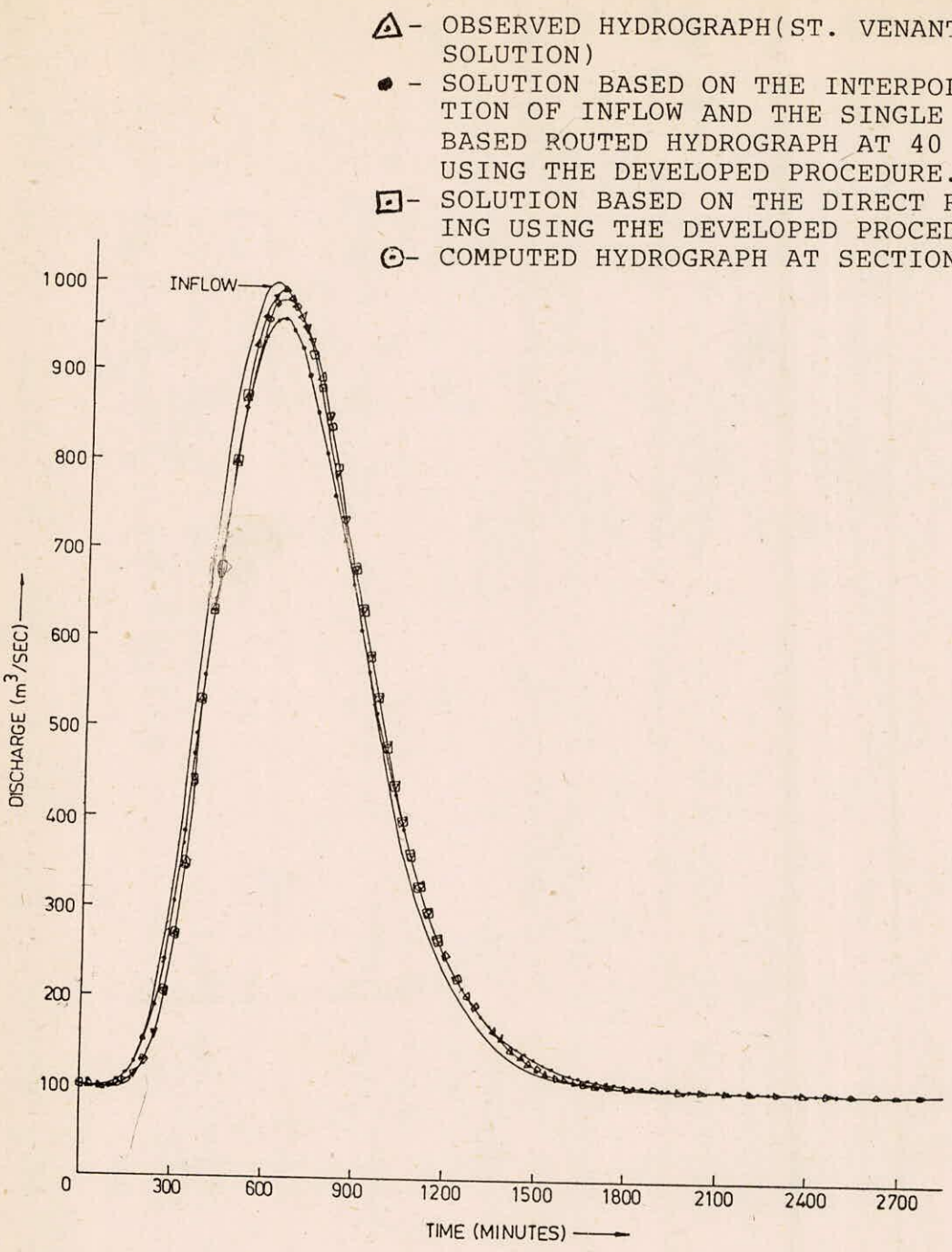

FIG.21 COMPARISON OF INTERPOLATED HYDROGRAPH AND DIRECTLY ROUTED HYDROGRAPH FOR 5 KM REACH (CHANNEL TYPE-2)

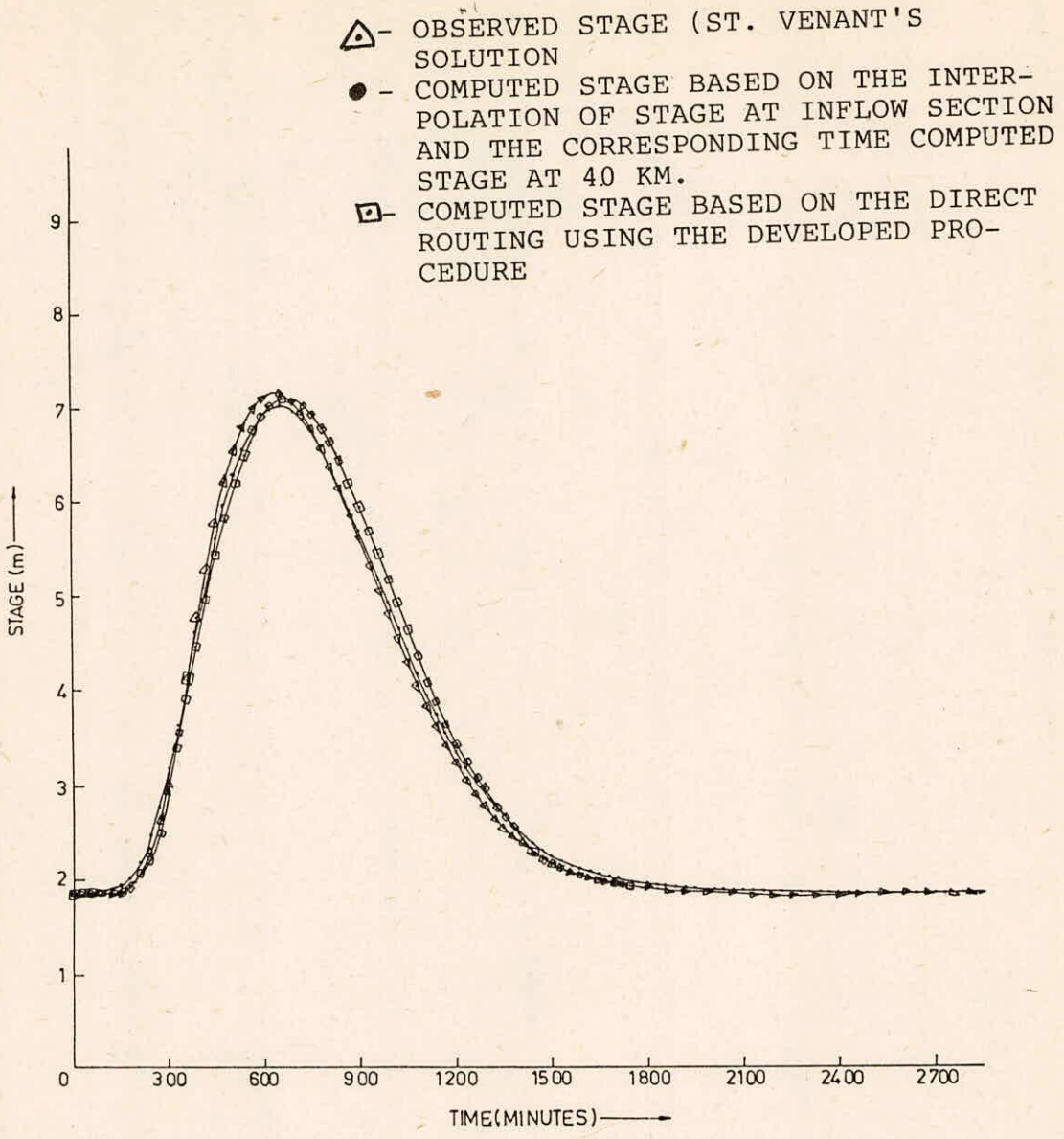

FIG.22 COMPARISON OF INTERPOLATED STAGE HYDROGRAPH AND THE STAGE HYDROGRAPH OBTAINED BY DIRECT ROUTING FOR 5 KM REACH (CHANNEL TYPE-2)

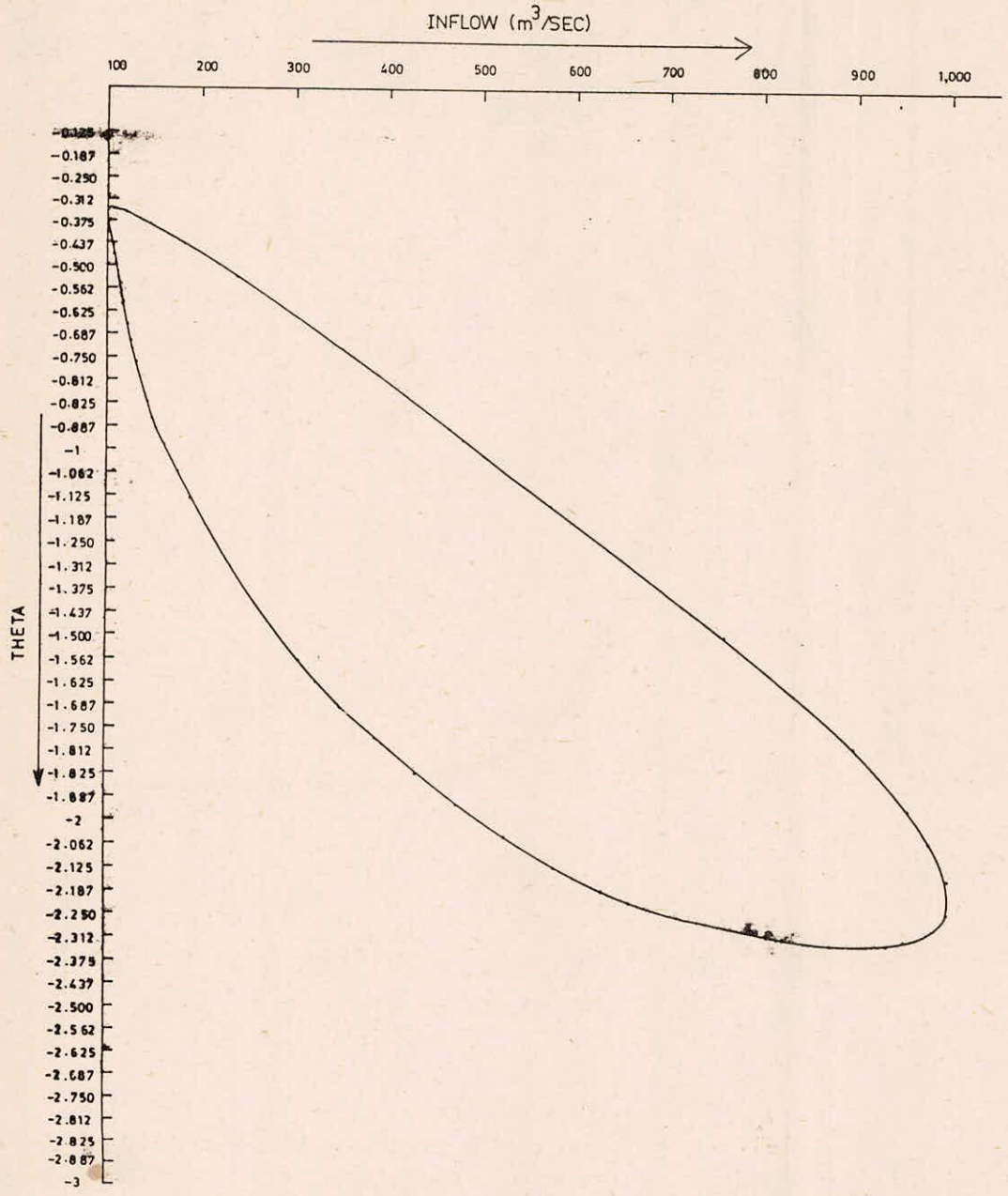

FIG.23 VARIATION OF Θ WITH INFLOW FOR THE ROUTING REACH OF 5 KM (CHANNEL TYPE-1)

6.2 Discussions

6.2.1 On the results of test run nos. (1),(2) and (3)

Based on the consideration of variance explained, it can be seen from Table-3 and verified from figure (3), that the hydrograph computed corresponding to test run no. 1 is able to reproduce the St. Venant's solution more closely than the solutions of test run nos. 2 and 3, except at the beginning of routing. The computed hydrograph dips in the beginning as observed by many researchers (Nash, 1959; Venetis, 1969; and Dooge, 1973) in the case of Muskingum flood routing method. The reasoning for this dip is explained at a later stage.

The hydrograph of test run no.2, corresponding to the case of constant θ and varying K, does not reproduce the St. Venant's solution satisfactorily. The constant θ value estimated for this test run was 0.3198 and it was obtained using the expression given by equation (77) after freezing all the flow variable with reference to the reference discharge Q_o which was computed as (Price, 1973):

$$Q_o = \frac{I_p + Q_p}{2} \qquad \ldots(97)$$

where,

I_p = the inflow hydrograph peak

Q_p = the outflow hydrograph peak

The reasoning for the weighting parameter becoming negative is given later. Note that the value of Q_p required for the computation of Q_o was unknown and it was approximately considered as the peak value of the hydrograph obtained by routing

the given inflow hydrograph for the same reach length using varying K and that θ value which was computed from equation (77) based on initial flow conditions. It may be noted from Table-3 that conservation of mass principle is grossly violated in this case when compared with the cases of test run nos. 1 and 3. However both test run nos. 1 and 2 reproduce equally well, the other characteristics of hydrographs such as error in peak flow and stage value, and the errors in time to peak discharge and stages.

The results of test run nos. 1 and 3 are better than test run no.2 from the aspect of conservation of mass. While dip in the beginning of routing was observed in the case of test run nos. 1, it was absent in the computed hydrograph of test run no. 3. Although the peak flow was slightly underestimated in the case of test run no. 3 (690 m^3/sec. when compared with 758 m^3/sec observed; and 740 m^3/sec obtained from test run No.1), the other hydrograph characteristics were well reproduced especially the stage hydrograph. It has to be noted that there was no computational problem faced in the case of test run no.3 of channel type-I when the reach of 40 km. was sub-divided into 8 sub-reaches as it was noted in the corresponding rectangular case(Perumal, 1986-87). It may be inferred from the overall considerations of results presented in Table-3 for these three runs, that the routing solution obtained from eight sub-reaches consideration may be preferable than the other two cases especially for flood forecasting purposes.

6.2.2 On the results of test run nos. (4),(5) and (6)

As seen from Table-3, the variance explained by the solution approaches of test nos. 4 and 6 were greater than 99%. Similarly in both cases, the conservation of mass was well maintained ($\leqslant 0.25\%$). However the multiple reach solution with 8 sub-reaches and Δx = 5 km., belonging to test run no.6, performed well when compared with the results of test run no.4 in reproducing the stage hydrograph. Note that the peak stage was differing from the true solution only by 0.05 m. when compared with 0.32 m of test run no.4. The variance explained by the solution procedure of test run no. 5 is less than that of the other two cases, although the difference is not significant. However from the consideration of conservation of mass, this test case performed poorly than the other two cases. In this aspect, the performance was similar to that of test run no.2 which also used the varying K and constant θ solution approach in arriving at the routed hydrograph at 40 km. Therefore the routing of steep rising inflow hydrographs such as in the cases of test run no. (2) and (5), in very flat streams, using constant θ and varying K based solution approach may not yield appropriate results. However further studies are required to arrive at any definite conclusion about this statement.

Considering the result of test run nos. (4), (5) and (6), one may prefer again the multiple reach based solution allowing both the parameters K and θ to vary.

6.2.3 On the results of test run nos. (7),(8)and (9), and (10), (11) and (12)

In all these runs the variance explained by the different

solution approaches was greater than 99% with the absolute maximum error in the conservatioin of mass being = 0.42%. All the other hydrograph characteristics were very well reproduced. These test runs results indicated that there was no significant difference between the results of variable parameters solution approach in which both θ and K varying; the solution approach based on the variatioin of K only keeping θ constant; and number of sub-reaches solution approach considering the variation of both θ and K. As will be discussed later, that there exists no significant variation of θ values corresponding to the given inflow ordinates for the test run nos. (7) and (9) of channel type-3, and test run nos. (10) and (12) of channel type-4. In these cases the value of $\frac{1}{S_o} \cdot \frac{\partial y}{\partial x}$ was nearer to zero indicating that the flood wave is of kinematic in nature. This inference has been verified by figures (7) and (9) as there was very little attenuation of flood peaks in these cases. It may be inferred from the closeness of the solutions shown by figures (7) and (9) that the method suggested herein may be used for kinematic routing of flood wave in long reaches in a single step routing.

6.2.4 On the results of test run nos. (13),(14),(15) and (16)

Test Nos. 13 and 14 were conducted on channel type-1 and these 15 and 16 were conducted on channel type-II. These tests were conducted for the verification of interpolatioin solution obtained at 5 km. distance from the inflow point using the hydrographs at the inflow section and the computed outflow hydrographs, obtained based on single reach routing solution,

at 40 Km. The verification was made by comparing the interpolation solution at 5 Km. with the corresponding direct routing solution based on the same solution approach. It can be seen from table-3 that the results of these runs are comparable to each other and also they are well comparable with the St. Venant's solution. The same may be verified from figures 19,20 21 and 22. It may be inferred from the results of these test runs that the unsteady flow solution required at any section of the reach may be obtained by linear interpolation of the inflow hydrograph and the resulting routed outflow hydrograph of a long reach obtained in a single step solution. This interpolation approach replaces the number of tedious routing computations for short reaches. The basic difference between test run nos. 13 and 14, and 15 and 16 is with reference to the value of Manning's roughness coefficient of the channel. While n = 0.04 for test run no. 13 and 14 it was 0.02 for the latter test runs. Results of latter runs indicate better performance than the former runs which may be attributed to the reduction in the roughness coefficient which indirectly causes the reduction in the magnitude of water surface slope and thus making it possible to adhere closely to the assumptions involved in the development of the procedure.

6.2.5 On the variation of K and θ

Variation of K :

Figure (11),(12),(13) and (14) show the variations of the travel time parameter K at each routing time level with reference to the corresponding time level inflow ordinates for

the cases of test run nos. (1),(4),(7)and(10). The purpose of relating K with the inflow hydrograph ordinates is to assess the real variation of K for all channel configurations studied, standing on a common platform such as the inflow hydrograph which is not influenced by the outflow information based on this method. Note that in all these cases the reach length Δx was fixed as 40 km. It can be seen from these figures that for all the cases the travel time corresponding to the same inflow discharge decreases as the order of channel type increase which implies that the velocity increases with the increase in the order of channel types. The reduction in the magnitude of K in the case of channel type-2, when compared with channel type-1 is solely due to reduction in Manning's roughness coefficient to 0.02, when compared with the corresponding value of 0.04 in the case of channel type-1. As indicated by figures (13) and (14) the increase in the bed slope also causes increase in the velocity. Therefore this discussion confirms that the physics of the open channel flow, i.e. the decrease in roughness coefficient or increase in bed slope or both cause increase in the velocity of flow, is closely followed by the methodology presented herein. It has been seen that the travel time in trapezoidal channel is slightly greater than that in the rectangular channel(Perumal 1986-87) for the same inflow discharge.

Variation of θ

Figures (15),(16),(17)and(18)show the variations of the weighting parameter θ at each routing time level with

reference to the corresponding time level inflow ordinates for the cases of test run nos. (1),(4),(7) and (10). Before discussing these results, it is necessary to look into the aspects of the variation of θ from the physical point of view.

The weighting parameter θ can be expressed as:

$$\theta = \frac{1}{2} - \frac{\ell}{\Delta x} \qquad \ldots(98)$$

With reference to figure (2), θ represents the non-dimensional distance between section (3) and (2). Using equation (98), the variation of θ can be studied.

When section (3) lies between the mid-section and the outflow section of the routing reach, $0<\theta<0.5$. When section(3) coincides with section (2), then $\theta = 0$ as in the Kalin-Milyukov method.

However if the routing reach length is such that section (2) is located ahead of section (3), in whcih case $\ell>\frac{\Delta x}{2}$, the value of $\theta<0$. When such a situation occurs during the routing process using this procedure, the outflow discharge magnitude would be greater than the normal discharge Q_3 as observed at section (3).

This situation was experienced in test run no. (13) in which the θ values corresponding to each time level of routing was negative and thus the outflow discharge was greater than the normal discharge Q at all the time levels of routing. Figure(19) shows the discharge hydrograph results of test run no. 13, in which the single reach solution obtained by varying both θ and K is plotted along with the St. Venant's solution. The corresponding normal discharge hydrograph is also shown

therein. It can be seen from this plot, that the outflow discharge hydrograph is observed ahead of normal discharge hydrograph confirming the interpretations based on equation (98). It was observed that $-2.3301 \leq \theta \leq -0.3294$ for this case. Although the possibility of $\theta < 0$ was indicated by Dooge (1973), the argument in favour of θ becoming negative from physical point of view has been put forwarded by Strupczewski and Kundzewicz (1980). Note that the value of $\theta < 0$ does not have any meaning in the case of Muskingum-Cunge method as it is considered as the numerical weighting factor with $0 < \theta < 1$. From the point of view of numerical mathematics as generally understood for the flood routing application $\theta \not< 0$. Therefore the reasoning given herein for $\theta < 0$ makes the present theory more attractive than any other theories presented so far on the Muskingum flood routing method.

When section (3) coincides with the mid-section, i.e., $\ell = 0$ and this leads to $\theta = \frac{1}{2}$. This represents the situation in which the normal discharge coincides with the normal depth at the mid-section of the reach and thus leading to the Kinematic flood wave movement.

The situation wherein $\theta > 0.5$, implies the location of section (3) upstream of mid-section of the routing reach and based on the physical basis of the model, i.e., the discharge proceedes the corresponding steady flow stage in unsteady flow situation, the change of direction of flow could be realized. Accordingly, the computed hydrograph at the outflow section i.e, at section (2), would be the amplification of the inflow

hydrograph. Explanations on the basis of various considerations are also available for $\theta > 0.5$ by other researchers (Cunge, 1969; Dooge, 1973; and Strupczwski and Kundzewicz, 1980).

It can be seen from figures (15) and (16) which belong to test run nos. (1) and (4) respectively, that the variation of θ w.r.t. inflow ordinates are wider. However for test run nos. (7) and (10), the variation of θ was not very much and their values were also found to be nearer to 0.5. These variations are brought out in figures (17) and (18). However, the θ values in these runs are greater than the corresponding values in rectangular channel (Perumal 1986-87).

It can be inferred from these variations that when the term $\frac{1}{S_o} \cdot \frac{\partial y}{\partial x}$ is nearer to zero and its variation is not significant then the value of θ is nearer to 0.5 and its variation is less. But when the magnitude of $\frac{1}{S_o} \cdot \frac{\partial y}{\partial x}$ is large and varies much, it causes wider variations in the value of θ including the possibility of θ values becoming negative as shown in figure(23) corresponding to test run no. 13. An understanding of these variations as explained above can be obtained from equation (46) and (47). The term $\frac{1}{S_o} \cdot \frac{\partial y}{\partial x}$ is inversely proportional to the term $v_m \cdot \frac{\partial A}{\partial y}\big|_m$ and therefore, higher magnitude of $\frac{1}{S_o} \cdot \frac{\partial y}{\partial x}$ implies lower magnitude of $v_m \frac{\partial A}{\partial y}\big|_m$ which in multiplication with S_o results in the higher value of 'ℓ' the distance between mid-section and section (3) of the routing reach. Thus the magnitude of θ will be much less than 0.5. When $\frac{1}{S_o} \cdot \frac{\partial y}{\partial x}$ is nearer to zero, there is increase in the magnitude of $v_m \frac{\partial A}{\partial y}\big|_m$ and this causes decrease in the value of 'ℓ'. Thus the

magnitude of θ will be nearer to 0.5. The typical values of the terms $\frac{1}{S_o} \cdot \frac{\partial y}{\partial x}$ as calculated using this methodology for test runs nos. (1), (4) (7) and (10) have been tabulated below:

TABLE 4

TYPICAL VALUE OF $\frac{1}{S_o} \cdot \frac{\partial y}{\partial x}$

Sl.No.	Test Run No.	Channel Type	Length of Reach	No. of Reaches	Magnitude of $\frac{1}{S_o} \frac{\partial y}{\partial x}$		Remarks
					Minimum	Maximum	
1	1	1	40 km	1	-0.6694	0.4558	Single reach
2	3	1	40 km	8	-1.2253	1.1908	first reach
					-0.7991	0.7928	second reach
					-0.7860	0.6563	third reach
					-0.7706	0.5657	fourth reach
					-0.7535	0.5010	fifth reach
					-0.7359	0.4520	sixth reach
					-0.7166	0.4131	seventh reach
					-0.6959	0.3812	eight reach
3	4	2	40km	1	-0.3949	0.2435	single reach
4	7	3	40 km	1	-0.0281	0.0143	single reach
5	10	4	40 km	1	-0.0142	0.0062	single reach

It can be seen from Table-4 that the typical value of $\frac{1}{S_o} \cdot \frac{\partial y}{\partial x} > 1$ for test run no. (3) and for this situation the binomial series expansion is not convergent even though the results obtained are not very poor from the true values. Further, it can be seen as the order of channel type increases, the typical values of $\frac{1}{S_o} \cdot \frac{\partial y}{\partial x}$ become less and less indicating that the attenuation causing factors do not have any role to play in the routing process.

It was observed while discussing the results of test

run no. (3) in section 6.2.1, that the eight sub-reaches solution with both θ and K varying resulted in the stage hydrograph much closer to that of St. Venant's solution when compared with the case of single reach solution with both θ and K varying. This is due to the assumption of linear variation of water surface is closely followed in eight sub-reaches solution case than in the case of single reach solution. Therefore to follow the assumption of linear variation of $\frac{\partial y}{\partial x}$, it is necessary to subdivide the reaches into smaller reaches. At this juncture, one may rise the question that why the discharge hydrograph of test run no. (3) was not properly estimated in the case of eight sub-reaches solution when compared with the discharge hydrograph of single reach solution. The reason may be attributed to the magnitude of $\frac{1}{S_o} \frac{\partial y}{\partial x} > 1$ as observed in the first reach of the eight sub-reaches solution, thus invalidating the solution of discharge hydrograph from the first reach. When this hydrograph is routed along the sub-reach, the resulting hydrograph is poorly estimated than the single reach solution. From these discussions one can infer that the assumption of linear variation of discharge is more valid than the assumption of linear variation of flow depth for a longer routing reach.

6.2.6 On the cause of dip in the beginning of solution.

This physically based routing method enables to ascertain the cause of negative or reduced or dip in the beginning of solution of the Muskingum flood routing method in the following manner:

The governing unsteady flow equation of the Muskingum

method is given as:

$$I - Q = \frac{d}{dt}[K(\theta I + (1-\theta)Q] \qquad \ldots(8)$$

Multiplying both sides of equation (8), by $(1-\theta)$ gives:

$$I-(\theta I+ (1-\theta)Q) = \frac{d}{dt}[K(1-\theta)\ (\theta I + (1-\theta)Q)] \qquad \ldots(99)$$

But the expression $\theta I + (1-\theta)Q$ is same as Q_3 , the normal discharge.

Therefore equation (99) is re-written as:

$$I - Q_3 = \frac{d}{dt}[K(1-\theta)Q_3] \qquad \ldots(100)$$

The solution of equation (100) assuming K and θ to be constant, yields :

$$Q_3 = \frac{e^{-t/K(1-\theta)}}{K(1-\theta)} \int_o^t Ie^{\tau/K(1-\theta)}d\tau + I_o e^{-t/K(1-\theta)} \qquad \ldots(101)$$

When $I = I_o$ at $t = 0$

$$Q_3 = \frac{e^{-t/K(1-\theta)}}{K(1-\theta)} \int_o^t Ie^{\tau/K(1-\theta)}d\tau \text{ when } I=0 \text{ at } t=0 \qquad \ldots(102)$$

Equation (101) and (102) indicate that at section (3), $Q_3=I_o$ and $Q_3 = o$ respectively when $t = 0$. Since the discharge varies linearly along the reach from $t = 0$ onwards, this leads to a discharge less than I or O at section (2) when it is located downstream of section (3) for which case $0<\theta<0.5$. The discharge at section (2) would be always greater than the initial steady flow if it is located upstream of section (3) for which case $\theta < 0$. The above inference arrived based on constant θ and K is also valid for variable K and θ. Note that when ' ℓ ' is small and section (2) is located far away downstream of section(3), then such a situation leads to dip or negative flow in the be-

ginning of routing. The larger distance between sections (2) and (3) is due to longer reach considered for routing. This aspect has been brought out by the results of test run nos. (1) (4), (7) and (10) wherein the routing was carried out by considering 40 km. length of the channel as a single reach. the respective discharge and stage hydrographs plotted in figures (3)-(9) show the dip in the beginning of the solution.

The magnitude and duration of this dip depends on the magnitude of the terms $\frac{1}{S_o} \cdot \frac{\partial y}{\partial x}$. When the magnitude of this terms is high, then the magnitude and duration of the dip increases. This inference can be verified from the typical values of $\frac{1}{S_o} \cdot \frac{\partial y}{\partial x}$ given in Table-4 for runs (1), (4),(7) and (10) and from the respective stage and discharge hydrographs given in figures (3)-(10). The hydrograph solutions obtained for the above mentioned runs and for the same length of reach, after dividing it into sub-reaches, are also depicted in figures (3)-(10). These solutions indicate no dip in the beginning of routing and thus confirm the above inference arrrived regarding the formation of dip and its elimination.

7.0 CONCLUSIONS

1. A variable parameter simplified hydraulic method has been developed for routing floods in channel reaches having uniform trapezoidal cross-section and constant bed slope.
2. The governing equations of this method which describe the flood wave movement in channels are same as that of Muskingum flood routing method introduced by McCarthy (1938), and it has been demonstrated using this method that these equations can directly account for flood wave attenuation without attributing to it the numerical property of the method as stated by Cunge (1969). Therefore this method gives a new insight into the theoretical aspects of the Muskingum flood routing method.
3. The parameters θ and K of the Muskingum method have been related to the channel and flow characteristics.
4. The nonlinear behaviour of flood wave movement in channels having uniform trapezoidal cross-section may be modelled using this method by varying the parameter θ and K at every routing time level, but still adopting the linear form of solution equation.
5. There exists a minimum routing reach length for which this method with both θ and K varying can be applied successfully without experiencing computational problem due to high negative value of θ.
6. The flood routing solution in reaches having length less than the above mentioned minimum reach length, can be obtained by linear interpolation of discharge and stage

hydrographs of given inflow hydrographs and the corresponding computed outflow hydrographs obtained at the location of minimum reach length using this variable parameters method.

7. In general, the method in which both θ and K varying along with multiple routing reaches consideration is able to reproduce the true solution much closer than the method in which both θ and K varying, but with the consideration of single routing reach.
8. In general, the method in which both θ and K varying is able to reproduce the true solution much closer than the method in which only K varying and θ remaining constant.
9. However when the relative water surface slope $\frac{1}{S_o} \cdot \frac{\partial y}{\partial x}$ is very small, there is no difference between the solutions obtained using the method in which both θ and K varying, and the method in which only K varying and θ remaining constant.
10. As there is no standard definition of "small" and "large" applicable with regard to the magnitude of the relative water surface slope $\frac{1}{S_o} \cdot \frac{\partial y}{\partial x}$, it is always desirable to use this routing method with the consideration of multiple routing reaches, and both parameters θ and K varying in each reach routing.
11. The higher the absolute magnitude of the relative water surface slope $\frac{1}{S_o} \cdot \frac{\partial y}{\partial x}$, the higher the values of travel time K and their variation for the given channel cross-

section.

12. The higher the absolute magnitude of the relative water surface slope $\frac{1}{S_o} \cdot \frac{\partial y}{\partial x}$, the higher the variation of weighting parameter θ.
13. The weighting parameter θ would be negative when section (2) is located upstream of section (3) at any instant of time during routing.
14. The cause of reduced outflow in the beginning of routing solution of Muskingum method is due to the linear variation of discharge considered by the method over the routing reach and due to longer routing reach length Δx considered for routing.
15. The magnitude and duration of reduced outflow is directly proportional to the magnitude of the relative water surface slope $\frac{1}{S_o} \cdot \frac{\partial y}{\partial x}$, and the length of routing reach Δx.
16. To avoid this reduced outflow theoretically, the routing reach should be divided in such a manner that section (2) is located upstream of section (3) for each considered sub-reach.
17. Routing in uniform rectangular channels can be achieved using this procedure by putting $Z = 0$ in the governing equations for the parameter K and θ.

REFERENCES

1. Apollov, B.A., G.P. Kalinin, and V.D. Komarov (1964), "Hydrological Forecasting", (Translated from Russian), Israel Program for Scientific Translations, Jerusalam.

2. Cunge, J.A. (1969), " On the subject of a Flood Propagation Method (Muskingum Method); ' Journal of Hydraulic Research, IAHR, Vol. 7, No.2, pp. 205-230.

3. Dooge, J.C.I. (1973), "Linear Theory of Hydrologic Systems,." Technical Bulletin No. 1468, Agriculatural Research Service USDA, Washington.

4. Dooge, J.C.I., W.G. Strupczewski, and J.J. Napiorkowski (1982), "Hydrodynamic Derivation of Storage parameters of Muskingum Model. "Journal of Hydrology, Vol. 54, pp. 371-381.

5. Fread, D.L. (1981), "Flood Routing: A Synopsis of Past, Present and Future Capability", In : Singh (Editor), Rainfall-Runoff Relationship, Proceedings of the International Symposium on Rainfall-Runoff Modelling, Mississippi State University, U.S.A.

6. Harley, B.M. (1967), "Linear Routing in Uniform Open Channel", M. Engg. Sc. Thesis, National University of Ireland (Unpublished).

7. Henderson, F.M. (1966), " Open Channel Flow" MacMillan and Co., New York, 1966.

8. Hyami, S. (1951), " On the Propagation of flood Waves; "Bull.1, Disaster Prevention Research Institute, Kyoto Univ., Japan.

9. Keefer, T.N. and R.S. McQuivey, (1974), "Multiple Linearization Flow Routing Model", Journal of the Hydraulic Division, ASCE, Vol. 100, No. HY7, pp. 1031-1046.

10. Koussis, A.D. (1978), " Theoretical Estimation of Flood Routing Parameters", Journal of the Hydraulics Division, ASCE, Vol. 104, No. HY1, pp 109-115.

11. Kundzewicz,Z. (1986), " Physically Based Hydrological Flood Routing Method,: Hydrological Sciences-Journal, 31, 2, 6.

12. Lighthill, M.J., and G.B. Whitham (1955), "On Kinematic Waves-I", Proc, Roy. Soc. A., Vol. 229, pp. 281-316.

13 McCarthy, G.T. (1938), "The unit hydrograph and Flood Routing", presented at Conf. North Atlantic Div., U.S. Army Corps of Engineers (Unpublished).

14. Meyer, O.H. (1941), "Simplified Flood Routing", Civil Engineering Vol. 11, No. 5, pp. 396-397.

15. Miller, W.A. and J.A. Cunge (1975), "Simplified Equations of Unsteady Flow", In:K Mahmood and V. Yevjevich (Editors), Unsteady Flow in Open Channel, Vol. I, Water Resources Publication, Forth Collins, Colorado, U.S.A.

16. Nash, J.E. (1959), " A note on the Muskingum Method of flood Routing", Journal of Geophysical Research, Vol. 64, pp. 1053-1056.

17. NERC, (1975), "Flood Studies Report-III Flood Routing Studies", London, England.

18. Perumal, M. (1986-87), "Development of a variable parameter Simplified Hydraulic Flood Routing Model for Rectangular Channels", TR-13, National Institute of Hydrology, Roorkee, India.

19. Ponce, V.M., and V. Yevjevich, "The Muskingum-Cunge Method with Variable Parameters", Journal of the Hydraulics Division ASCE, Vol. 104, No. Hy. 12, pp. 1663-1667.

20. Price, R.K. (1973), "Flood routing Methods for British Rivers", Hydraulics Research Station, Wallingford, INT 111, 102 p.

21. Strupczewski, W., and Z. Kundzewics (1980),"Muskingum Method Revisited,", Journal of Hydrology, Vol. 48, pp. 327-342.

22. Thomas, I.E., and P.R. Wormleaton (1970), "Flood Routing Using a Convective-Diffusion Model", Civil Engineering and Public Works Review Vol. 65, pp. 257-259.

23. Venetis, C. (1969), " The IUH of the Muskingum Channel Reach,", Journal of Hydrology, Vol.7, pp.444-447.

24. Weinmann, P.E. (1977), "Comparison of Flood Routing Methods for Natural Rivers", Report No. 2/1977, Deptt. of Civil Engineering, Monash University, Victoria, Australia.